

**DESIGN AND ANALYSIS OF DIELECTRIC RESONATOR
ANTENNA FOR ULTRAWIDE BAND AND Ka BAND
APPLICATIONS**

A THESIS

**SUBMITTED IN PARTIAL FULFILLMENT OF THE
REQUIREMENTS FOR THE DEGREE OF
MASTER OF TECHNOLOGY**

IN

ELECTRONIC SYSTEMS AND COMMUNICATION

BY

CHANDRA KANDULA

Roll No. – 210EE1220



Department of Electrical Engineering

National Institute of Technology

Rourkela-769008

2012-13

**DESIGN AND ANALYSIS OF DIELECTRIC RESONATOR
ANTENNA FOR ULTRA WIDE BAND AND Ka BAND
APPLICATIONS**

A THESIS

**SUBMITTED IN PARTIAL FULFILLMENT OF THE
REQUIREMENTS FOR THE DEGREE OF
MASTER OF TECHNOLOGY**

IN

ELECTRONIC SYSTEMS AND COMMUNICATION

BY

CHANDRA KANDULA

Roll No. – 210EE1220

UNDER THE GUIDANCE OF

PROF. P K SAHU



Department of Electrical Engineering

National Institute of Technology

Rourkela-769008

2012-13

Department of Electrical Engineering
National Institute of Technology Rourkela

CERTIFICATE

This is to certify that the thesis entitled, “**Design and Analysis of Dielectric Resonator Antenna for Ultra Wide Band and Ka Band applications**” submitted by *Mr. Chandra Kandula* in partial fulfillment of the requirements for the award of Master of Technology Degree in electrical Engineering with specialization in “**Electronic systems and communication**” during session 2010-2013 at the National Institute of Technology, Rourkela (Deemed University) is an authentic work carried out by him under my supervision and guidance.

To the best of my knowledge, the matter embodied in the thesis has not been submitted to any other University/ Institute for the award of any degree or diploma.

Date:

Prof. P K Sahu

Department of Electrical Engineering
National Institute of Technology
Rourkela-769008

Acknowledgment

This project work is by far the most significant accomplishment in my life and it would be impossible without people who supported me and believed in me.

I would like to express my deep sense of gratitude to **Prof. P.K. Sahu** for his invaluable help and guidance during the course of project. I am highly indebted to him for constantly encouraging me by giving his critics on my work. I am grateful to him for having given me the support and confidence. His trust and support inspired me in the most important moments of making right decisions and I am glad to work with him. My special thanks go to **Prof. A K Panda** Head of the Department of Electronics and Communications Engineering, NIT Rourkela, for providing us with best facilities in the Department and his timely suggestions.

I want to thank all my teachers **Prof. Susmitha Das, Prof. Dipti Patra** and **prof. K R Subhashini** for providing a solid background for my studies and research thereafter. They have been great sources of inspiration to me and I thank them from the bottom of my heart.

I would like to thank all my friends and especially my classmates for all the thoughtful and mind stimulating discussions we had, which prompted us to think beyond the obvious. I have enjoyed their companionship so much during my stay at NIT Rourkela. I would like to thank all those who made my stay in Rourkela an unforgettable and rewarding experience.

Last but not least I would like to thank my parents, who taught me the value of hard work by their own example. They rendered me enormous support during the whole tenure of my stay in NIT Rourkela.

Chandra Kandula

May 2013

National Institute of Technology, Rourkela

Abstract

Here the design of a simple and a generic transmission line (T.L.) circuit approach along with a fast and generic formulation for the novel antenna model is developed. The proposed antenna is a specific shaped placed on a material of dielectric constant of ϵ equal to 4.4(FR 4) and size of 26mm×28mm. The ϵ (epsilon) value of dielectric resonator is taken to be 2.1 (material: Teflon). A simple micro strip line feeding of novel design has been used to feed the antenna. The ground plane is considered to be 26mm×11.7mm in size. The proposed antenna is simulated and a return loss of -10db below is obtained which is in the range of 3.67 GHz to 9.18 GHz. The proposed DRA can cover maximum frequency range of the UWB band. The Directivity of the antenna is simulated to be 9.054dbi .The proposed antenna can be used for UWB wireless networks.

In a similar way the design of an another DR antenna having specific shape and a generic transmission line (T.L.) circuit approach along with a fast and generic formulation for the novel antenna model is developed. The proposed antenna is modeled as an I-shape and is placed on a material of dielectric constant of ϵ equal to 2.2(Teflon material) and size of 15mm×11mm. The ϵ (epsilon) value of dielectric resonator is taken to be 10.2 (material: Rogers RO3010). A simple micro strip line feeding of novel design has been used to feed the antenna. The ground plane is considered to be 10mm×11mm in size. The proposed antenna is simulated and a return loss of -10db below is obtained which is in the range of 30.58 GHz to 39 GHz. Here a good return loss is obtained at two peaks whose values are -21db at 31.54 GHz and a value of -22db at 35.39 GHz. In this paper a bandwidth improvement of 24.36% has been achieved. In addition to that a total efficiency of 72.88% is found at 35.39 GHz and 69% is found at 31.54 GHz. A directivity of 10.2dbi at 35.39 GHz and a 7.61dbi at 31.54 GHz have been claimed, besides that a significant gain of 10.59db at a frequency of 35.39 GHz and 8.34db at 31.54 GHz. The designed antenna is proposed for applications in the area of satellite communications, radio location, and imaging systems for weapon and hazardous material detection.

CONTENTS

Chapter No.	Topic Name	Page No.
1	INTRODUCTION	1
	Thesis Overview	2
	1.1 Introduction	2
	1.2 Thesis Motivation	4
	1.3 Thesis Outline	5
2	ANTENNA PARAMETERS	6
	2.1 Antenna Parameters	7
	2.1.1 Directivity	7
	2.1.2 Gain	7
	2.1.3 Bandwidth	7
	2.1.4 Voltage Standing Wave Ratio (VSWR)	8
	2.1.5 Antenna Polarization	8
	2.1.6 Input impedance	9
	2.1.7 Quality factor	10
3	ULTRA-WIDE BAND AND MILLIMETER WAVE OVERVIEW	11
	3.1 ULTRA WIDEBAND OVERVIEW	12
	3.1.1 Key Benefits Of UWB	12
	3.1.2 Application areas for UWB	13
	3.2 Millimeter Wave Overview	13
	3.2.1 Key Benefits Of Millimeter Wave	16
	3.2.2 Application areas for Millimeter Wave	16

4	DIELECTRIC RESONATOR ANTENNA	18
	4.1 Dielectric Resonators	19
	4.1.1 Common Applications Of DRO	19
	4.2 Historical Overview	19
	4.3 Investigations on Dielectric resonator antenna	20
	4.4 Advantages over Micro Strip Antennas	21
	4.5 Characteristics of the Dielectric Resonator Antennas	22
	4.6 Excitation Methods Applied To The DRA	23
	4.7 Materials for dielectric resonators	24
	4.8 Method of analysis	24
	4.9 Analyses of the DRA	25
	4.9.1 Resonant frequencies	25
	4.9.2 Equivalent magnetic surface currents	27
	4.10 Basic cylindrical DRA Simulation results	29
5	COUPLING TO DRAs	31
	5.1 Coupling Coefficients	32
	5.2 Fields Within Rectangular and Cylindrical DRAs	35
	5.3 Aperture Coupling	39
	5.4 Probe Coupling	49
	5.5 Micro strip Line Coupling	55
	5.6 COPLANAR COUPLING	57
	5.7 DIELECTRIC IMAGE GUIDE COUPLING	58
	5.8 SURVEY OF ANALYTICAL METHODS	59
	5.8.1 Frequency Domain Analysis	60
	5.8.2 Time Domain Analysis Techniques	61

6	ANTENNA DESIGN AND MEASUREMENT RESULTS	63
	6.1. Introduction	64
	6.2 Design and Analysis of I-shape dielectric resonator antenna	65
	6.3 Simulation results and discussions	66
	6.3.1 Reflection coefficient (S11)	66
	6.3.2 Voltage standing wave ratio	67
	6.3.3 Radiation directivity, gain patterns	68
	6.4 Design of UWB Antenna	69
7	CONCLUSIONS AND FUTURE SCOPE	75
	7. 1. Conclusions	76
	7.2 Future Work	77
	Publication(s)	78
	References	79

List of Figures

Sl.No:	Fig. No.:	Figure Name	Page No.:
1	2.1	Typical variation of resistance and reactance of rectangular micro strip antenna versus frequency	9
2	3.1	UWB spectrum overlay	12
8	3.2	Average atmospheric gaseous attenuation of millimeter-wave propagation at sea level.	15
9	4.1	DRA s of various shapes.	21
10	4.2	Photos of a probe-fed DRA. (a) Above the ground plane are the coaxial probe and DRA. (b) Below the ground plane is the SMA connector for the coaxial probe. Normally the probe is inside the DRA	23
11	4.4	The geometry of cylindrical DRA.	24
12	4.5	Schematic view of cylindrical DRA	29
13	4.6	Simulated return loss versus Frequency of the cylindrical DRA	30
3	5.1	Sketch of the fields for the rectangular DRA	36
4	5.2	Sketches of the E-fields for selected higher-order modes within the rectangular DRA.	38
5	5.3	Sketch of the cylindrical DRA field configurations	41
7	5.4	Various slot apertures	42
6	5.5	Equivalent magnetic current for slot apertures	43
8	5.6	Slot apertures coupling to a rectangular DRA	44
18	5.7	Slot apertures coupling to a cylindrical DRA	45
19	5.8	Slot apertures coupling to a split-cylindrical DRA	46
20	5.9	Micro strip-fed rectangular slots	47
21	5.10	Vertical probe sources	50
14	5.11	Probe coupling to a rectangular DRA.	51
15	5.12	Probe coupling to the HE ₁₁ mode of the cylindrical DRA	53

16	5.13	Probe coupling to split-cylindrical DRAs	53
17	5.14	coupling to the TM ₀₁ mode of the cylindrical DRA	54
22	5.15	Micro strip line coupling to DRAs	55
23	5.16	Fields and equivalent radiation models of micro strip line-coupled DRAs.	56
24	5.17	Various coplanar feeds for coupling to DRAs.	57
25	5.18	coplanar loops coupling to a cylindrical DRA	58
26	5.19	Dielectric image guide feed for DRAs	59
27	6.1	Geometry of the proposed I-shape DRA	66
28	6.2	Simulated reflection coefficient (Return Loss) for the proposed I-shape DRA versus frequency.	67
29	6.3	Simulated VSWR for the proposed antenna	67
30	6.4	surface current flow of the proposed antenna at frequency 35.39GHz	68
31	6.5	3-D view radiation pattern of the directivity of proposed DRA at frequency 35.39GHz	68
32	6.6	3-D view radiation pattern of the Gain of proposed DRA at frequency 35.39GHz.	69
33	6.7	Design of UWB antenna	69
34	6.8	Return loss graph of the antenna	70
35	6.9	Fabricated DR antenna for UWB applications	71
36	6.10	Measured return loss of the antenna	72
37	6.11	VSWR plot of the antenna	72

38	6.12	Measured value of VSWR	73
39	6.13	Directivity plot of the antenna	73
40	6.14	polar representation of directivity	74
41	6.15	E- field pattern ($\phi=90$)	74

CHAPTER 1

INTRODUCTION

1.1 INTRODUCTION

Satellite communication and Wireless communication have been developed rapidly in the past decades and it has already a dramatic impact on human life. In the last few years, the development of wireless local area networks (WLAN) represented one of the principal interests in the information and communication field. The field of wireless communications has been undergoing a revolutionary growth in the last decade. This is attributed to the invention of portable mobile phones some 15 years ago. The success of the second generation (2G) cellular communication services motivates the development of wideband third generation(3G) cellular phones and other wireless products and services, including wireless local area networks, home RF, Bluetooth, wireless local loops, local multi-point distributed networks (LMDS), to name a few. The crucial component of a wireless network or device is the antenna. Very soon, our cities will be flooded with antennas of different kinds and shapes. On the other hand, for safety and portability reasons, low power, multi-functional and multiband wireless devices are highly preferable. All these stringent requirements demand the development of highly efficient, low-profile and small-size antennas that can be made embedded into wireless products.

In the early 1960s, researchers from Columbia University, Okaya and Barash, reported the first ever DR in the form of a single crystal TiO. In the mid-1960s, Cohn and his coworkers at Rantec Corporation performed the first extensive theoretical and experimental evaluation of DR. Nevertheless, the DR was still far from being used in practical applications. A real breakthrough in the dielectric ceramic industry occurred in the early 1970s when Masse et al developed the first temperature-stable, low-loss barium tetratitanate ceramics. In 1975, Van Bladel reported detailed theory to evaluate the modes of DR.

Dielectric resonators (DRs), made of low loss dielectric materials, are widely used in various applications. They are compact in size, low in cost and weight and could be excited using different transmission lines. Dielectric materials with dielectric constant values in the range of 10–100 have been used in applications at microwave frequencies. The high relative permittivity at the interfaces of DR and free space provides a standing electromagnetic wave inside the resonator. Besides the high dielectric constant and low loss, the stable temperature coefficient of these advanced materials offer new design opportunities for microwave applications. DRAs offer simple coupling schemes to nearly all transmission lines used at microwave and millimeter-wave frequencies. This makes them suitable for integration into different planar technologies. The coupling between a DRA and the planar transmission line can

be easily controlled by varying the position of the DRA with respect to the line. The performance of DRA can therefore be easily optimized experimentally. The operating bandwidth of a DRA can be varied over a wide range by suitably choosing resonator parameters. For example, the bandwidth of the lower order modes of a DRA can be easily varied from a fraction of a percent to about 10% or more by the suitable choice of the dielectric constant of the resonator material.

DRs of different shapes have various modes of oscillation. With the proper excitation of certain modes and with no shielding, these resonators can actually become efficient radiators instead of energy storage devices. This concept led to the exploration of DRs as antennas. Although open DRs were found to radiate many years ago, the idea of using DR as a practical antenna materialized in 1983, when Long et al published a paper on cylindrical dielectric resonator antennas (DRAs). Subsequently, other researchers investigated rectangular and hemispherical DRAs. These works laid the foundation for later extensive investigations on various aspects of DRAs. Considerable work done on analyzing their resonant modes, radiation characteristics, and various feeding schemes has demonstrated that these “new” radiators could offer new and attractive features in antenna design.

In the last 2 decades, two classes of novel antennas have been investigated and extensively reported on. They are the micro strip patch antenna and the dielectric resonator antenna. Both are highly suitable for the development of modern wireless communications. Since Federal communications commission (FCC) has announced the UWB frequency range from 3.1 GHz to 10.6 GHz the investigations on these two types of novel antennas increased rapidly.

The aim of the thesis is to design and simulate dielectric resonator antenna for wireless millimeter wave(band)applications (from 30 to 300 gigahertz) and the designing the dielectric resonator antenna for Ultra-wide band applications (from 3.6 GHz to 9 GHz) and study the effects of antenna dimensions, substrate thickness on the Radiation parameters of Bandwidth for both the cases.

I have implemented this particular antenna using CST software. There are a few soft wares available which allow the design optimization of the antenna. CST microwave studio is one of the most imperial electromagnetic software which allows to solving for radio and microwave application. CST MICROWAVE STUDIO® is a fully featured software package for

electromagnet IC analysis and design in the high frequency range. It simplifies the process of inputting the structure by providing a powerful solid modeling front-end which is based on the famous ACIS modeling kernel. Strong graphic feedback simplifies the definition of your device even further. After the component has been input, a fully automatic meshing procedure (based on an expert system) is applied before the simulation engine is started. The simulator itself features the new Perfect boundary approximation (PBA method) and its Thin Sheet Technique (TST) extension, which increases the accuracy of the simulation by an order of magnitude in comparison to conventional simulators. Since no method works equally well in all application domains, the software contains four different simulation techniques (transient solver, frequency domain solver, Eigen mode solver, modal analysis solver) which best fit their particular applications. The "original" solver in CST Microwave Studio is based on Finite Integration Technique. The simulator tool computes most of the useful quantities of interest such as radiation pattern, reflection coefficient, voltage standing wave ratio (VSWR) and gain etc.

1.2 Thesis Motivation

The main motivation of this work is now day, mobile communication systems are becoming increasingly popular. Antennas for software-defined and / or reconfigurable radio systems need to have ultra-wide band or multi-band characteristics in order to be flexible enough to cover any possible future mobile communication frequency bands. One approach to provide such flexibility is to construct multi-band antenna that operates over specific narrowband frequencies. However, it would be extremely difficult to accurately achieve the frequency requirements of all future communication system. Alternatively, a small wideband antenna that covers a wide range of frequencies can be a good candidate not only for current multi-band applications but also for future communication systems operating on new frequency bands. With bandwidths as low as a few percent, wide band applications using conventional micro strip patch designs and dielectric resonator antenna (DRA) designs are limited. Other drawbacks of patch antennas include low efficiency, limited power capacity, spurious feed radiation, poor polarization purity, narrow bandwidth, and manufacturing tolerance problems.

To overcome these problems for over two decades, research scientists have developed several methods to increase the bandwidth and low frequency ratio of a patch antenna and dielectric resonator antenna (DRA). The motivation to extend dielectric resonator antenna for millimeter

applications is due to the dimension of a DRA. Thus by choosing a high value of ϵ_r (10-100), the size of the DRA can be significantly reduced. There is no inherent conductor loss in dielectric resonators. This leads to high radiation efficiency of the antenna. This feature is especially attractive for millimeter (mm)-wave antennas, where the loss in metal fabricated antennas can be high. Many of these techniques involve adjusting the placement and/or type of element used to feed (or excite) the antenna. Wide band frequency operation of antennas has become a necessity for many applications. Micro strip antennas and DRAs are ultimately expected to replace conventional antennas for most applications.

- Requirements for the digital home include high-speed data transfer for multimedia content, short-range connectivity for transfer to other devices
- Satellite communication system
- Radar and Imaging
- Medical Applications
- Location and Tracking
- Vehicular Radar Systems
- Low Data Rate and Low Power UWB Communications

1.3 Thesis Outline

The outline of this thesis is as follows.

Chapter 2: In this chapter the basics of antenna parameters such as radiation pattern, Impedance, VSWR, Gain, Directivity, Bandwidth, antenna polarization, Quality factor etc.

Chapter 3: Introduction to Ultra-wide band antenna, key benefits of UWB, applications and introduction to millimeter wave antenna, key benefits of millimeter wave, applications are presented.

Chapter 4: Introduction to Coupling, Types of Coupling.

Chapter 5: This chapter introduces the dielectric resonator antenna and the advantages over micro strip antenna, general characteristics and method of analysis of basic circular cylindrical DRA.

Chapter 6: Design of DR antenna for UWB applications and Ka band applications.

Chapter 7: Conclusions and Future scope.

CHAPTER 2

ANTENNA PARAMETERS

2.1 BASIC ANTENNA PARAMETERS

2.1.1 Directivity

Therefore directivity of an antenna defined as “the ratio of the radiation intensity in a given direction from the antenna to the radiation intensity averaged over all directions. The average radiation intensity is equal to the total power radiated by the antenna divided by 4π . If the direction is not specified, the direction of maximum radiation intensity is implied. Stated more simply, the directivity of a non isotropic source is equal to the ratio of its radiation intensity in a given direction over that of an isotropic source.

2.1.2 Gain

The gain of an antenna is the radiation intensity in a given direction divided by the radiation intensity that would be obtained if the antenna radiated all of the power delivered equally to all directions. The definition of gain requires the concept of an isotropic radiator; that is, one that radiates the same power in all directions. An isotropic antenna, however, is just a concept, because all practical antennas must have some directional properties. Nevertheless, the isotropic antenna is very important as a reference. It has a gain of unity ($G = 1$ or $G = 0$ dB) in all directions, since all of the power delivered to it is radiated equally well in all directions.

Although the isotopes are a fundamental reference for antenna gain, another commonly used reference is the dipole. In this case the gain of an ideal (lossless) half wavelength dipole is used. Its gain is 1.64 ($G = 2.15$ dB) relative to an isotropic radiator. The gain of an antenna is usually expressed in decibels (dB). When the gain is referenced to the isotropic radiator, the units are expressed as dBi; but when referenced to the half-wave dipole, the units are expressed as dBd. The relationship between these units is

$$G_{dBd}G_{dBd}=G_{dBi}G_{dBi}-2.15G_{dBd} \quad (2-1)$$

2.1.3 Bandwidth

The bandwidth of an antenna is defined as “the range of frequencies within which the performance of the antenna, with respect to some characteristic, conforms to a specified standard.” The bandwidth can be considered to be the range of frequencies, on either side of a center frequency (usually the resonance frequency for a dipole), where the antenna characteristics (such as input impedance, pattern, beam width, polarization, side lobe

level, gain, beam direction, radiation efficiency) are within an acceptable value of those at the center frequency. For broadband antennas, the bandwidth is usually expressed as the ratio of the upper-to-lower frequencies of acceptable operation [1].

2.1.4 Voltage Standing Wave Ratio (VSWR)

The standing wave ratio (SWR), also known as the voltage standing wave ratio (VSWR), is not strictly an antenna characteristic, but is used to describe the performance of an antenna when attached to a transmission line. It is a measure of how well the antenna terminal impedance is matched to the characteristic impedance of the transmission line. Specifically, the VSWR is the ratio of the maximum to the minimum RF voltage along the transmission line. The maxima and minima along the lines are caused by partial reinforcement and cancellation of a forward moving RF signal on the transmission line and its reflection from the antenna terminals.

If the antenna terminal impedance exhibits no reactive (imaginary) part and the resistive (real) part is equal to the characteristic impedance of the transmission line, then the antenna and transmission line are said to be matched. It indicates that none of the RF signal sent to the antenna will be reflected at its terminals. There is no standing wave on the transmission line and the VSWR has a value of one. However, if the antenna and transmission line are not matched, then some fraction of the RF signal sent to the antenna is reflected back along the transmission line. This causes a standing wave, characterized by maxima and minima, to exist on the line. In this case, the VSWR has a value greater than one. The VSWR is easily measured with a device and VSWR of 1.5 is considered excellent, while values of 1.5 to 2.0 is considered good, and values higher than 2.0 may be unacceptable.

2.1.5 Antenna Polarization

Polarization of an antenna in a given direction is defined as “the polarization of the wave transmitted (radiated) by the antenna. Polarization of a radiated wave is defined as “that property of an electromagnetic wave describing the time-varying direction and relative magnitude of the electric-field vector. If the E-field vector retains its orientation at each point in space, then the polarization is linear; if it rotates as the wave travels in space, then the polarization is circular or elliptical. In most cases, the radiated-wave polarization is linear and either vertical or horizontal. At sufficiently large distances from an antenna, beyond 10 wavelengths, the radiated, far-field wave is a plane wave.

2.1.6 Input impedance

Input impedance is defined as “the impedance presented by an antenna at its terminals or the ratio of the voltage to current at a pair of terminals or the ratio of the appropriate components of the electric to magnetic fields at a point”. Typically the feed reactance is very small, compared to the resonant resistance, for very thin substrates. However, for thick elements the reactance may be significant and needs to be taken into account in impedance matching and in determining the resonant frequency of a loaded element.

The most efficient coupling of energy between an antenna and its transmission line occurs when the characteristic impedance of the transmission line and the terminal impedance of the antenna are the same and have no reactive component. When this is the case, the antenna is considered to be matched to the line. Matching usually requires that the antenna be designed so that it has a terminal impedance of about 50 ohms or 75 ohms to match the common values of available coaxial cable.

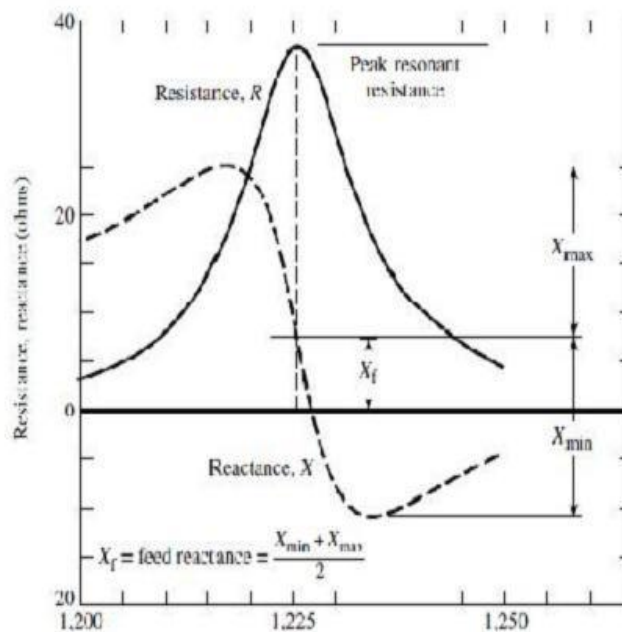


Figure 2.1 Typical variation of resistance and reactance of rectangular micro strip antenna versus frequency (Electromagnetism, Vol. 3, Nos. 3 and 4, p. 33, W. F. Richards, J. R. Zinecker, and R.D. Clark, Taylor & Francis, Washington, D.C).

In general, the input impedance is complex and it includes both a resonant and a non resonant part which is usually reactive. Both the real and imaginary parts of the impedance vary as a function of frequency and a typical variation is shown in Figure 2.1. Ideally both the resistance and reactance exhibit symmetry about the resonant frequency and the reactance at resonance is equal to the average of sum of its maximum value (which is positive) and its minimum value (which is negative).

2.1.7 Quality factor

The quality factor is a figure-of-merit that is representative of the antenna losses. Typically there is radiation, conduction (ohmic), dielectric and surface wave losses. Therefore the total quality factor Q_t is influenced by all of these losses and is, in general, written as

$$\frac{1}{Q_t} = \frac{1}{Q_{rad}} + \frac{1}{Q_c} + \frac{1}{Q_d} + \frac{1}{Q_{sw}} \quad (2-2)$$

Where

Q_t = total quality factor

Q_{rad} = quality factor due to radiation (space wave) losses

Q_c = quality factor due to conduction (ohmic) losses

Q_d = quality factor due to dielectric losses

Q_{sw} = quality factor due to surface waves

For very thin substrates, the losses due to surface waves are very small and can be neglected. However, for thicker substrates they need to be taken into account. These losses can also be eliminated by using cavities.

CHAPTER 3

ULTRA-WIDE BAND AND MILLIMETER WAVE OVERVIEW

3.1 ULTRA WIDEBAND OVERVIEW

Historically, UWB radar systems were developed mainly as a military tool. However, recently, UWB technology has been focused on consumer electronics and communications. Ideal targets for UWB systems are low power, low cost, high data rates, precise positioning capability and extremely low interference.

UWB technology is different from conventional narrowband wireless transmission technology – instead of broadcasting on separate frequencies; UWB spreads signals across a very wide range of frequencies. The typical sinusoidal radio wave is replaced by trains of pulses at hundreds of millions of pulses per second. The wide bandwidth and very low power makes UWB transmissions. In 1973 the first US patent was awarded for UWB communications. The field of UWB had moved in a new direction. Other applications, such as automobile collision avoidance, positioning systems, liquid-level sensing and altimetry were developed [26].

Ultra-Wideband (UWB) may be used to refer to any radio technology having bandwidth exceeding the lesser of 500 MHz or 20% of the arithmetic center frequency, according to 9 Federal Communications Commission (FCC). A February 14, 2002 Report and Order by the FCC authorizes the unlicensed use of UWB in the range of **3.1 to 10.6 GHz** [27].

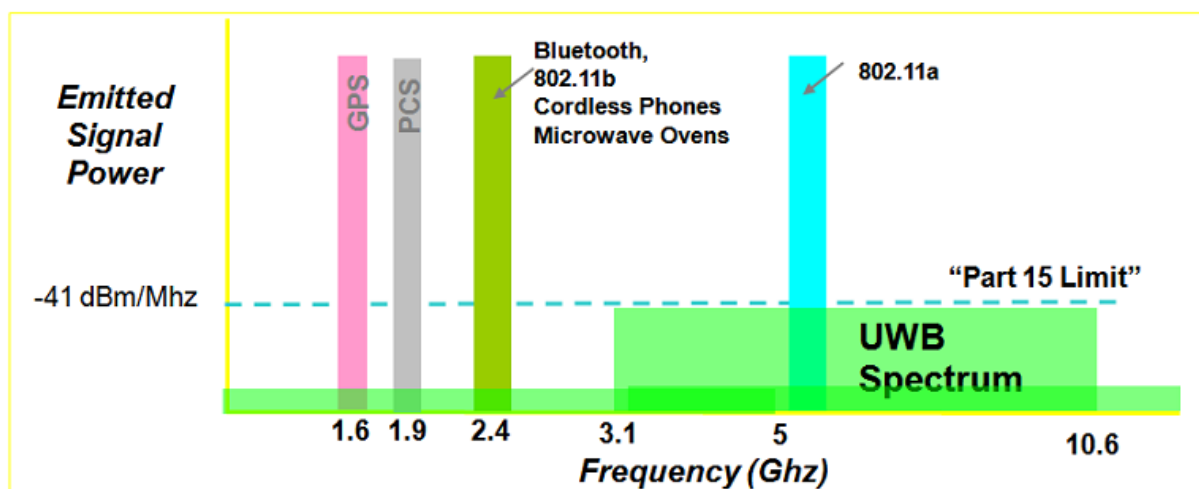


Figure 3.1 UWB spectrum overlay.

3.1.1 KEY BENEFITS OF UWB

The key benefits of UWB can be summarized as

1. High data rates

2. Low equipment cost
3. Multipath immunity
4. Ranging and communication at the same time

3.1.2 Application areas for UWB

- **Radar in Automotive Industry**

- **Security applications**

- Applications such as ground penetrating radar (GPR), through-wall surveillance, appear attractive given today's focus on detection.

- **Tracking applications**

- Applications involving the tracking of children, personnel, equipment and inventory, to an accuracy of less than one inch, are attractive, especially as UWB can work indoors (factories, shopping malls), unlike GPS.

- **Wireless Home Networks**

- Typically, a wireless home network should provide connection among various electronic consumer devices such as PC, MP3 player, digital camera, printer, scanner, High-Definition TV (HDTV) and video game console.

3.2 MILLIMETER WAVE OVERVIEW

Millimeter wave generally corresponds to the radio spectrum between 30 GHz to 300GHz, with wavelength between one and ten millimeters. However, in the context of wireless communication, the term generally corresponds to a few bands of spectrum near 38, 60 and 94 GHz, and more recently to a band between 70 GHz and 90 GHz (also referred to as E- Band), that have been allocated for the purpose of wireless communication in the public domain.

Though relatively new in the world of wireless communication, the history of millimeter wave technology goes back to the 1890's when J.C. Bose was experimenting with millimeter wave signals at just about the time when his contemporaries like Marconi were inventing radio communications. Following Bose's research, millimeter wave technology remained within the confines of university and government laboratories for almost half a century. The technology started to see its early applications in Radio Astronomy in the 1960's, followed by applications in the military in the 70's. In the 80's, the development of millimeter-wave integrated circuits created opportunities for mass manufacturing of millimeter wave products for

commercial applications.

In the 1990's, the advent of automotive collision avoidance radar at 77 GHz marked the first consumer-oriented use of millimeter wave frequencies above 40 GHz. In 1995, the FCC (US Federal Communications in the US, four bands in the upper millimeter wave region have been opened for commercial applications. Of the four bands, the 59-64 GHz band (commonly referred to as V-band or the 60GHz band) is governed by FCC Part 15 for unlicensed operations. The regulations of FCC Part 15 and the significant absorption of the 60 GHz band by atmospheric oxygen makes this band better suited for very short range point-to-point and point-to-multipoint applications. The 92-95 GHz band (commonly referred to as W-band or the 94 GHz band) is also governed by the FCC Part 15 regulations for unlicensed operation, though for indoor applications only. The 94 GHz band may also be used for licensed outdoor applications for point-to-point wireless communication per FCC Part 101 regulations. However the band is less spectrally efficient than the other three bands due to an excluded band at 94-94.1 GHz.

This leaves 71-76 GHz and 81-86GHz (commonly referred to as E-band or the 70GHz and 80GHz bands, respectively), whose use in the US is governed by FCC Part 101 for licensed operation, as the most ideally suited millimeter wave band for point-to-point wireless communication applications. With the 5 GHz of spectrum available in each of these two bands, the total spectral bandwidth available exceeds that of all allocated bands in the microwave spectrum. Through the remainder of this paper, we confine our discussion to these two bands.

The 5 GHz of spectrum available in each sub-band of the E-band spectrum can be used as a single, contiguous transmission channel (which means no channelization is required), thereby allowing the most efficient use of the entire band. Even with simple modulation techniques such as OOK (On-Off-Keying) or BPSK (Binary Phase Shift Keying), throughput of 1 to 3 Gbps is achieved today in each sub-band of the spectrum, more than what can be achieved with more sophisticated, higher order modulation schemes in other bands of licensed spectrum. Migrating to such modulation techniques at E-band, even higher throughputs can be achieved. It is only a matter of sufficient market demand before such higher throughput millimeter wave links become a commercial reality.

In the past few years, the interest in the millimeter-wave spectrum at 30 to 300 GHz has drastically increased. The emergence of low cost high performance CMOS technology and low loss, low cost organic packaging material has opened a new perspective for system designers and service providers because it enables the development of millimeter-wave radio at the same cost structure of radios operating in the gigahertz range or less. In combination with available ultra-wide bandwidths, this makes the millimeter-wave spectrum more attractive than ever before for supporting a new class of systems and applications ranging from ultra-high speed data transmission, video distribution, portable radar, sensing, detection and imaging of all kinds.

While at a lower frequency the signal can propagate easily for dozens of kilometers, penetrate through construction materials or benefit from advantageous reflection and refraction properties, one must consider carefully the characteristics (in particular strong attenuation and weak diffraction) of the millimeter-wave propagation, and exploit them advantageously. The free-space loss (FSL) (after converting to units of frequency and putting them in decibel form) between two isotropic antennas can be expressed as [1]

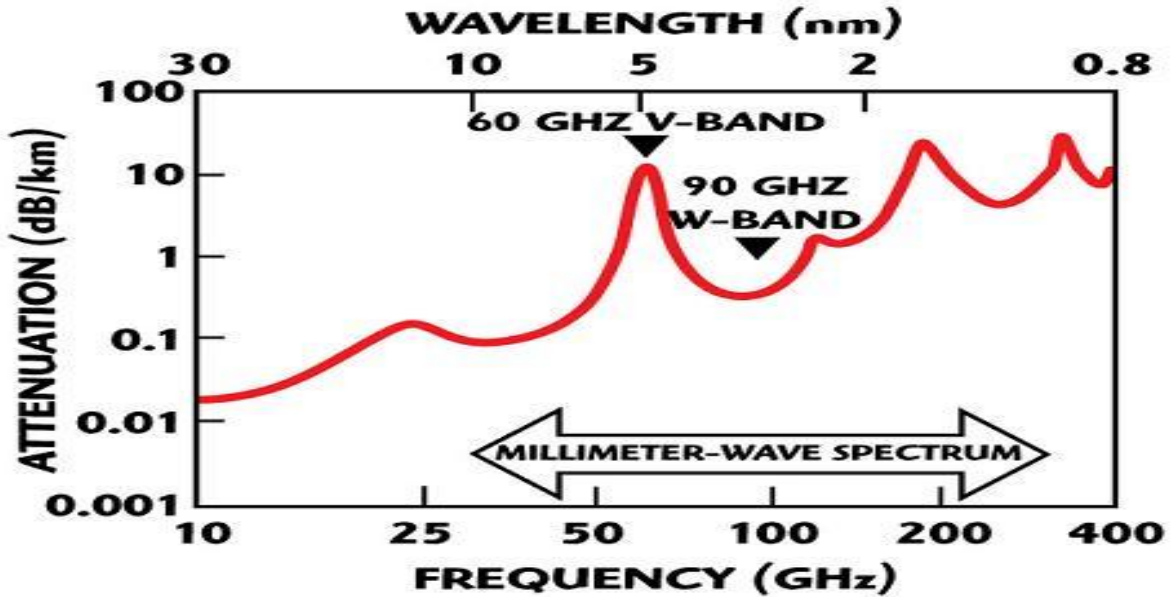


Figure 3.2 Average atmospheric gaseous attenuation of millimeter-wave propagation at sea level.

$$FSL = 92.4 + 20 \log F + 20 \log D$$

Where

F = frequency in gigahertz and

D = line-of-sight distance in kilometers

As an example, at 60 GHz the free-space loss is much more severe than at the frequencies usually used for cell phone and wireless applications. The link budget at 60 GHz is 21 dB less than the one at 5 GHz under equal conditions. In addition, other loss and fading factors increasingly affect the millimeter-wave transmission, such as gaseous (see Figure 3.2), rain, foliage, and scattering and diffraction losses.

3.2.1 KEY BENEFITS OF MILLIMETER WAVE

The key benefits of MILLIMETER WAVE can be summarized as

1. Ultra-high speed data transmission
2. Unmatched Bandwidth with Scalable Capacity
3. Narrow Beam with Highly Scalable Deployments
4. Licensed Spectrum with Low Cost Licensing
5. Mature Technology with Multi-vendor Solutions
6. Detection and imaging of all kinds

3.2.2 Application areas for MILLIMETER WAVE

- **Metro Network Services**

With the economy becoming more information dependent, the bandwidth needs of corporations, large and small, continue to grow apparently without bound. However, a large majority of corporate buildings are still being served only by archaic copper wires barely able to deliver a few megabits per second of bandwidth.

- **Cellular/WiMAX Backhaul**

With the use of mobile handheld devices growing and newer bandwidth-intensive applications emerging, the need to deliver higher bandwidth to mobile users will continue to rise. As newer technologies such as WiMAX and new spectrum such as 700 MHz are used to serve these needs at the access point; the need for a technology to transport the bandwidth from the point of access to the core of the network will rise swiftly. To this day, most of those needs have been met by slower capacity channels such as T1/E1 leased lines. However, these solutions will not be able to meet the needs of the next generation of mobile networks in a practical manner.

- **Cellular Distributed Antenna Systems (DAS)**

In cellular networks, it is often necessary or more efficient to enhance network coverage by distributing a network of remote antennas instead of providing coverage by way of centrally located antennas. Such distributed antenna systems (DAS) are basically extensions of the antenna of base stations. DAS are often used to provide cellular coverage in spots that are shadowed by large structures, such as buildings, from base station antennas. DAS may also be used to provide coverage in areas where it is not efficient to install a base station.

- **Failure Recovery and Redundancy**

For applications requiring high end-to-end bandwidth, broadband connectivity by means of fiber optic cables is often the technology of choice when access to fiber optic cables is readily available. However, cases abound where fiber connections have been broken by accident, for instance during trenching operations, often bringing down mission critical networks for a substantial period of time. Therefore, it is highly desirable to design such mission critical networks with redundancies that minimize probability of such failures.

- **Enterprise and Campus Networks**

The needs of enterprises to extend LANs from one building to a neighboring building are often so compelling that users in such applications have been the earliest adopter of point-to-point wireless technologies. As organizations expand their facilities by growing in to neighboring buildings, the cost of leasing interconnecting communication services becomes significant, eventually persuading them to look for alternate solutions.

CHAPTER 4

DIELECTRIC RESONATOR ANTENNA

4.1 DIELECTRIC RESONATORS

Introduction:

A dielectric resonator (dielectric resonator oscillator, DRO) is an electronic component that exhibits resonance for a narrow range of frequencies, generally in the microwave band. The resonance is similar to that of a circular hollow metallic waveguide, except that the boundary is defined by large change in permittivity rather than by a conductor. Dielectric resonators generally consist of a "puck" of ceramic that has a large dielectric constant and a low dissipation factor. The resonance frequency is determined by the overall physical dimensions of the puck and the dielectric constant of the material.

Although dielectric resonators display many similarities to resonant metal cavities, there is one important difference between the two: while the electric and magnetic fields are zero outside the walls of the metal cavity (i.e. open circuit boundary conditions are fully satisfied), these fields are not zero outside the dielectric walls of the resonator (i.e. open circuit boundary conditions are approximately satisfied). Even so, electric and magnetic fields decay from their maximum values considerably when they are away from the resonator walls. Most of the energy is stored in the resonator at a given resonant frequency for a sufficiently high dielectric constant.

4.1.1 Common Applications of DRO

Most common applications of dielectric resonators are:

- filtering applications (most common are band pass and band stop filters)
- Oscillators (diode, feedback-, reflection-, transmission- and reaction-type oscillators).
- Frequency- selective limiters.
- DRA (Dielectric Resonator Antenna) elements.

4.2 Historical Overview

In the late 19th century, Lord Rayleigh demonstrated that an infinitely long cylindrical rod made up of dielectric material could serve as a waveguide. Additional theoretical and experimental work done in Germany in early 20th century, offered further insight into the behavior of electromagnetic waves in dielectric rod waveguides. Since a dielectric resonator can be thought of as a truncated dielectric rod waveguide, this research was essential

for scientific understanding of electromagnetic phenomena in dielectric resonators. In 1939

Robert D. Richtmyer published a study [15] in which he showed that dielectric structures can act just as metallic cavity resonators. He appropriately named these structures dielectric resonators. Richtmyer also demonstrated that, if exposed to free space, dielectric resonators must radiate because of the boundary conditions at the dielectric-to-air interface. These results were later used in development of Dielectric Resonator Antenna (DRA). Due to World War II, lack of advanced materials and adequate manufacturing techniques, dielectric resonators fell in relative obscurity for another two decades after Richtmyer's study was published. However, in 1960's, as high-frequency electronics and modern communications industry started to take off, dielectric resonators gained in significance. They offered a size-reducing design alternative to bulky waveguide filters and lower-cost alternatives for electronic oscillator, frequency selective limiter and slow-wave circuits. In addition to cost and size, other advantages that dielectric resonators have over conventional metal cavity resonators are lower weight, material availability, and ease of manufacturing.

4.3 INVESTIGATIONS on Dielectric resonator antenna

For many years, the dielectric resonator (DR) has primarily been used in microwave circuits, such as oscillators and filters, where the DR is normally made of high permittivity material, with dielectric constant $\epsilon_r > 20$. The unloaded Q-factor is usually between 50 and 500, but can be as high as 10,000. Because of these traditional applications, the DR was usually treated as an energy storage device rather than as a radiator. Although open DRs were found to radiate many years ago, the idea of using the DR as an antenna had not been widely accepted until the original paper on the cylindrical dielectric resonator antenna (DRA) [16] was published in 1983. At that time, it was observed that the frequency range of interest for many systems had gradually progressed upward to the millimeter and near-millimeter range (100-300 GHz). At these frequencies, the conductor loss of metallic antennas becomes severe and the efficiency of the antennas is reduced significantly.

Conversely, the only loss for a DRA is that due to the imperfect dielectric material, which can be very small in practice. After the cylindrical DRA had been studied, Long and his colleagues subsequently investigated the rectangular and hemispherical DRAs. The work

created the foundation for future investigations of the DRA. Other shapes were also studied, including the spherical-cap [17], and cylindrical-ring DRAs [18], triangular [19]. Figure 4.1 shows a photo of various DRAs. It was found that DRAs operating at their fundamental modes radiate like a magnetic dipole, independent of their shapes [8].

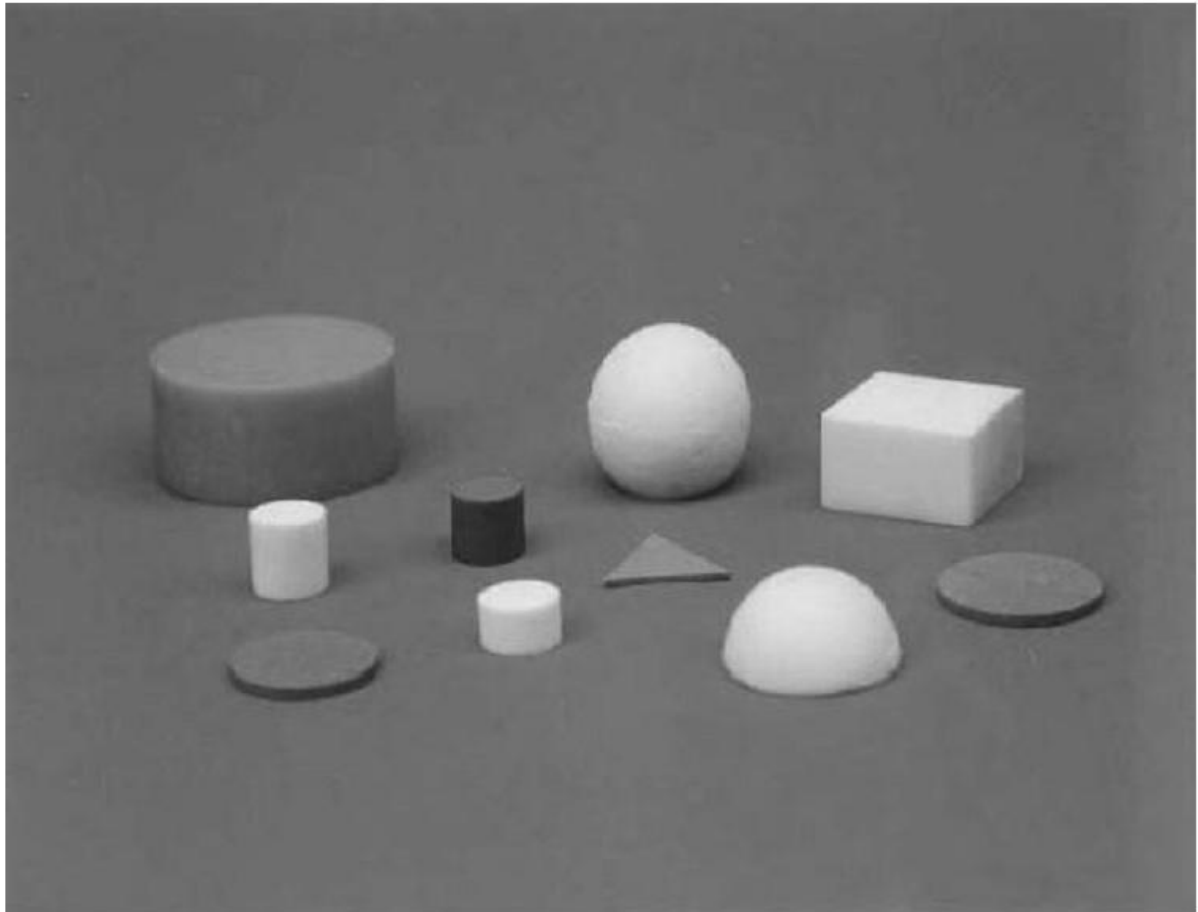


Figure 4.1 DRAs of various shapes. The photo shows cylindrical, rectangular, hemispherical, low profile circular-disk, low-profile triangular and spherical-cap DRAs [8].

4.4 Advantages over micro strip antennas

As compared to the micro strip antenna, the DRA has a much wider impedance bandwidth ($\sim 10\%$ for dielectric constant ~ 10). This is because the micro strip antenna radiates only through two narrow radiation slots. This is explained in chapter 3, whereas the DRA radiates through the whole DRA surface except the grounded part [20].

Avoidance of surface waves is another attractive advantage of the DRA over the micro strip antenna. Nevertheless, many characteristics of the DRA and micro strip

antenna are common because both of them behave like resonant cavities.

4.5 Characteristics of the Dielectric Resonator Antennas

For different applications the dielectric resonator has been studied extensively in recent years from low frequencies to high frequencies. The dielectric resonator antenna has versatility and high flexibility in adopting a shape over a wide frequency range, which allows the desired requirement to the designer. Some of the major advantages or characteristics of the dielectric resonator antenna are as follows:

- A millimeter-wave frequency operation can be achieved by choosing a low-loss characteristic dielectric material due to an absence of surface waves and minimal conductor losses associated with the dielectric resonator antenna. At these frequencies high radiation efficiency can be achieved [20].
- The dielectric constant ϵ can be from a range of below 3 up to 100.
- Different methods can be used to excite the dielectric resonator antenna (slot, probe, coplanar, micro strip, waveguide, dielectric image guide, etcetera.) which make them easy to integrate with the existing technologies [8].
- Dielectric resonator antennas are designed to operate over a wide frequency range of 1.3 GHz to 40 GHz [20].
- Dielectric resonator antennas have high dielectric strength which makes them capable to handle high power. This also helps them to work in a wide temperature range due to the temperature-stable ceramic materials.
- Many modes can be excited within the dielectric resonator antenna element depending on the shape of the resonator. Different modes give different radiation patterns for various coverage requirements.
- The radiation Q-factor of the modes depends on the aspect ratio; the aspect ratio is an important parameter in designing a dielectric resonator antenna because it gives one more degree of freedom for the design [20].
- The dielectric resonator antenna has much wider impedance bandwidth compared to the micro strip antenna. It is because the dielectric resonator antenna radiates through the whole antenna surface except for the ground whereas the micro strip antenna radiates only through the narrow slots [21].

The fabrication of dielectric resonator antennas is more complex and more costly

compared to printed circuit antennas, especially for array applications. Maybe for high-volume of production the cost reduces but the economic scale is not that important. The problem with dielectric resonator antennas is typically that ceramic materials which are machined to shape from a large block are used. To feed the antenna excitations from e.g. probes, the antenna needs to be drilled since it is bounded to a ground plane or a substrate. There are applications where performance is more important than cost and the dielectric resonator can antenna provide the solution.

4.6 Excitation methods applied to the DRA

A number of excitation methods have been developed [1-4]. Examples are the coaxial probe, aperture-coupling with a micro strip feed line, aperture-coupling with a coaxial feed line, direct micro strip feed line, co-planar feed, soldered-through probe, slot line, strip line conformal strip, and dielectric image guide is shown in figure 4.3. A photo of the coaxial probe excitation scheme is shown in Figure 4.2. Some of the feeding methods are addressed in chapter 3, whereas the rigorous analyses of the aperture coupling with a perpendicular feed and conformal strip feed are presented. Virtually all excitation methods applicable to the micro strip antenna can be used for the DRA.

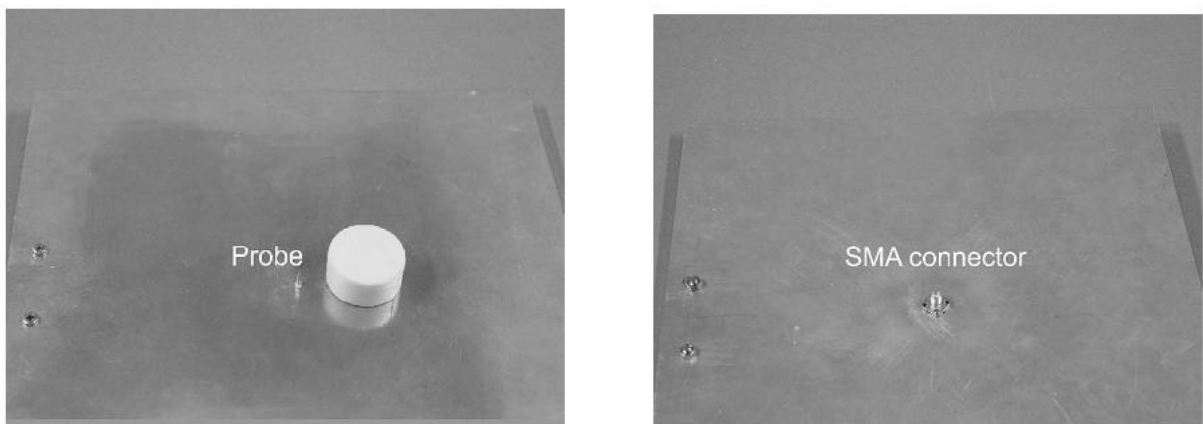


Figure 4.2 Photos of a probe-fed DRA. (a) Above the ground plane are the coaxial probe and DRA. (b) Below the ground plane is the SMA connector for the coaxial probe. Normally the probe is inside the DRA [8].

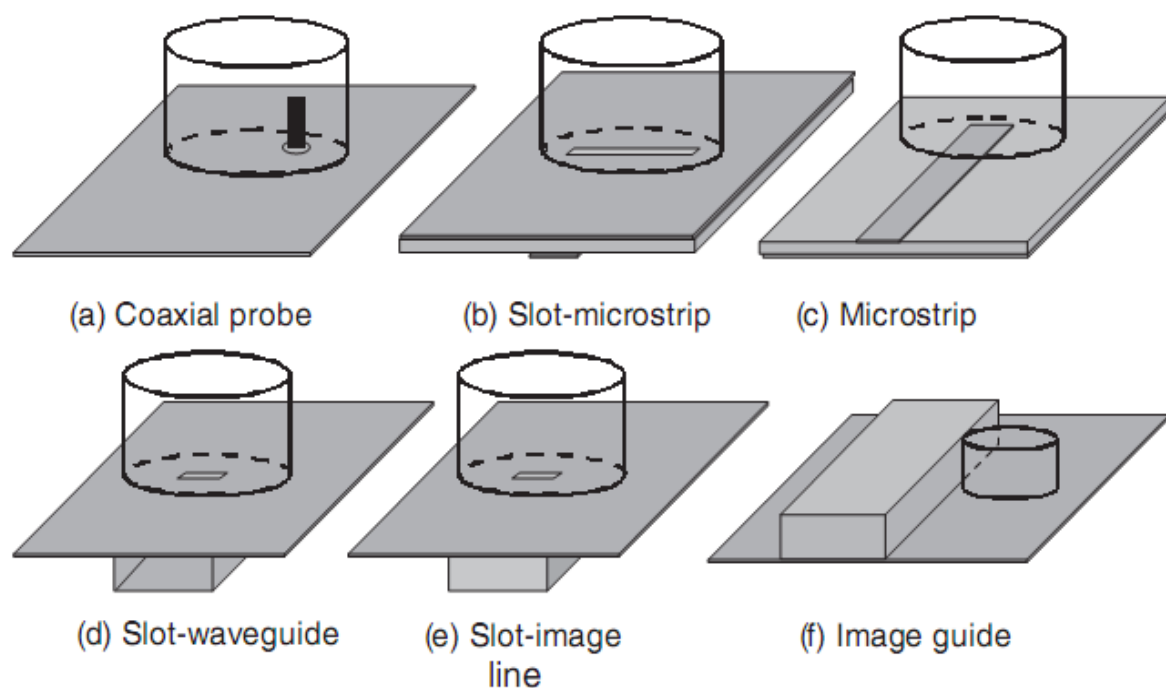


Figure 4.3 Different excitation mechanisms for the DRA

4.7 Materials for dielectric resonators

Different materials have Different applications and requirements of the dielectric resonator. The dielectric properties depend on the crystal structure, material, and imperfections in the crystal lattice as well as on the preparation conditions. Dielectric resonators generally consist of a puck-formed cylinder of ceramic material of high permittivity and low dissipation factor. Traditional passive devices have been desired to have a high Q-factor (up to 20,000 between 2 and 20GHz [21]), high permittivity and near zero temperature coefficients for the resonant frequency which has been difficult to achieve simultaneously. The low-permittivity ceramics have so far been used for millimeter-wave applications and also as substrates for microwave integrated circuits. Ceramics with permittivity in the range between 25 and 50 have been used for satellite communication and in cell phone base stations. High permittivity materials are used in mobile telephones, where the compact size sets narrow limits. In all the mentioned cases the use has been for circuit components. Materials of lower relative permittivity are Teflon based plastic materials. One provider of these materials is the Rogers Corporation, with sheets of materials with permittivity from around 2 to 10.2.

4.8 Method of analysis

There is no exact analytic solution to the Maxwell's equations for many of the

complicated structures of the dielectric resonators that are used as antennas. In the beginning, when the radiation from the hydrogen atom was not understood, a method such as the Bohr planetary theory of the atom was used to predict the radiation spectra. The most popular modes to analyze DRAs are the magnetic wall model, the transmission line model and numerical methods (method of moments or finite elements). The magnetic line model and the transmission line model are good for building physical insight. However they are not as accurate as numerical methods. Numerical methods are the most accurate but they offer very little physical insight.

4.9 Analyses of the DRA

Cylindrical DRA

A simple analysis for the cylindrical DRA was carried out in [22] using the magnetic wall model. Figure 4.3 shows the DRA configuration, along with standard cylindrical coordinates.

4.9.1 Resonant frequencies

In the analysis, the DRA surfaces are assumed to be perfect magnetic conductors, with the feed probe temporarily ignored. For such a cavity, wave functions which are transverse electric (TE) to z and transverse magnetic (TM) to z can be written as

$$\Psi_{\text{TE}_{n\text{pm}}} = J_n \left(\frac{X_{np}}{a} \rho \right) \left\{ \begin{matrix} \sin n\phi \\ \cos n\phi \end{matrix} \right\} \sin \left[\frac{(2m+1)\pi z}{2d} \right] \quad (4-1)$$

$$\Psi_{\text{TM}_{n\text{pm}}} = J_n \left(\frac{X_{np}'}{a} \rho \right) \left\{ \begin{matrix} \sin n\phi \\ \cos n\phi \end{matrix} \right\} \cos \left[\frac{(2m+1)\pi z}{2d} \right] \quad (4-2)$$

where J_n is the Bessel Function of the first kind, with $J_n(X_{np})=0$, $J_n'(X'_{np})=0$, $n=1,2,3,\dots$, $p=1, 2, \text{ and } 3,\dots$, $m=0, 1, 2, 3,\dots$.

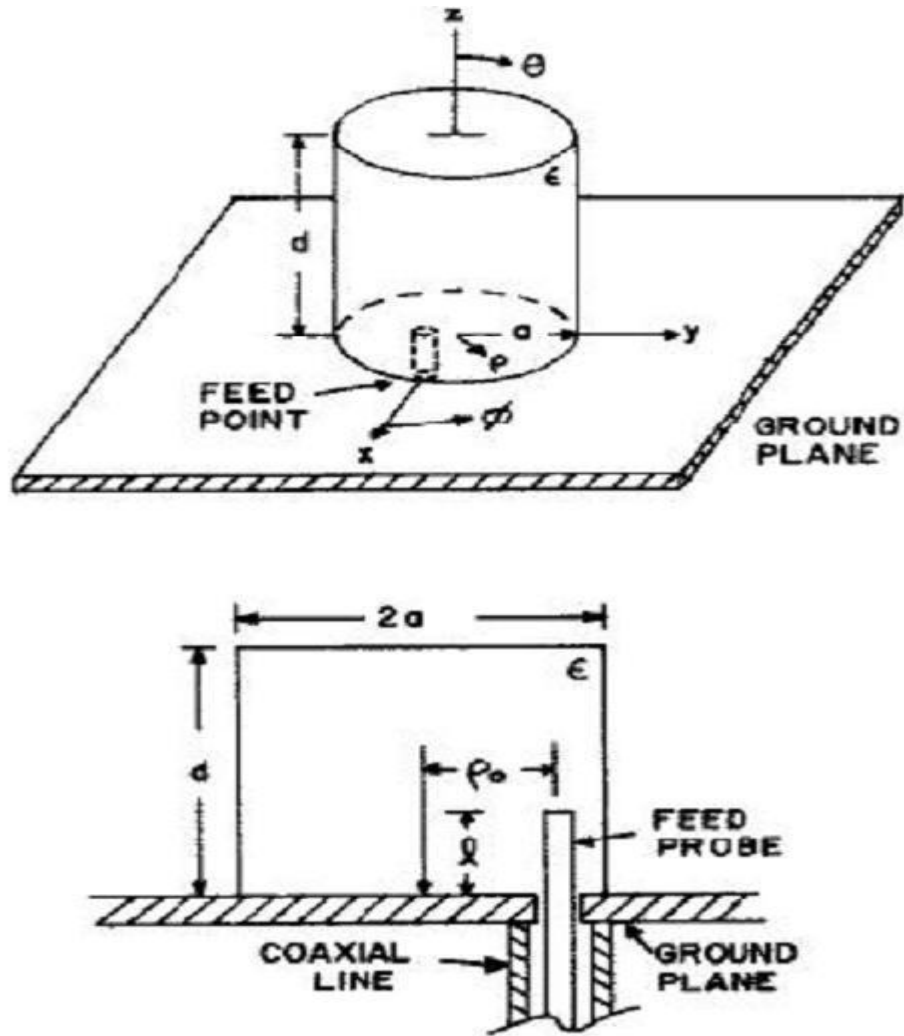


Figure 4.4 The geometry of cylindrical DRA. (From [22], © 1983 IEEE).

From the separation equation $k_p^2 + k_z^2 = k^2 = \omega^2 \epsilon$, the resonant frequency of the npm mode.

$$f_{n\pi m} = \frac{1}{2\pi a \sqrt{\mu \epsilon}} \sqrt{\left\{ \begin{matrix} X_{np}^2 \\ X_{np}'^2 \end{matrix} \right\} + \left[\frac{\pi a}{2d} (2m + 1) \right]^2} \quad (4-3)$$

$$f_{TM_{110}} = \frac{1}{2\pi a \sqrt{\mu \epsilon}} \sqrt{X_{11}'^2 + \left(\frac{\pi a}{2d} \right)^2} \quad (4-4)$$

Where $X'_{11} = 1.841$.

4.9.2 Equivalent magnetic surface currents

The TM_{110} mode fields inside the cylindrical DRA are used for the derivation of the far-field expressions. To begin, the wave function of the fundamental TM_{110} mode is found:

$$\psi_{TM_{110}} = \psi = J_n \left(\frac{X'_{11}}{a} \rho \right) \cos \phi \cos \left[\frac{\pi z}{2d} \right] \quad (4-5)$$

The $\cos \phi$ term is selected because the feed position is at $\phi = 0$. Conversely, the $\sin \phi$ term should be used if the probe is located at $\phi = \pi/2$. From the wave function, the various E-fields can be easily found:

$$E_{\phi} = \frac{1}{j\rho\omega\epsilon} \frac{\partial^2 \psi}{\partial \phi \partial z}$$

$$E_z = \frac{1}{j\omega\epsilon} \left(\frac{\partial^2}{\partial z^2} + k^2 \right) \psi$$

$$E_{\rho} = \frac{1}{j\omega\epsilon} \frac{\partial^2 \psi}{\partial \rho \partial z}$$

(4-6)

Use is made of the equivalence principle to find the equivalent magnetic currents on the DRA surfaces. The equivalent currents will be treated as the radiating sources for the

radiation fields. In the following expressions, the primed and unprimed coordinates are used to indicate the source and field, respectively. From $M = E \times \hat{n}$ where \hat{n} is a unit normal pointing out of the DRA surface, the following equivalent currents are obtained:

2. for the top and bottom

$$M'_Q = \frac{\pi X'_{11}}{2j\omega\epsilon_{ad}} J_1' \left(\frac{X'_{11}\rho'}{a} \right) \cos \phi' \quad (4-7)$$

$$M'_\rho = \frac{\pi}{2j\omega\epsilon_{d\rho}} J_1' \left(\frac{X'_{11}\rho'}{a} \right) \sin \phi' \quad (4-8)$$

4.10 Basic cylindrical DRA Simulation results

Here the basic cylindrical DRA was simulated with radius- to- height ratio $a/d = 0.3$. In this design we used cylindrical dielectric resonator having dielectric constant 8.9. The cylindrical DRA is excited by a micro strip line feed. The cylindrical dielectric resonator is supported by a square substrate having relative permittivity constant $\epsilon_r = 4.4$ with dimensions (LS \times WS) 80 mm \times 60 mm and height $h_s = 1.6$ mm. The dimensions of the ground plane are (Lg \times Wg) 30 mm \times 30 mm. Here the cylindrical resonator is with height $h_1 = 10$ mm and radius = 3 mm and it is placed at the centre of the substrate.

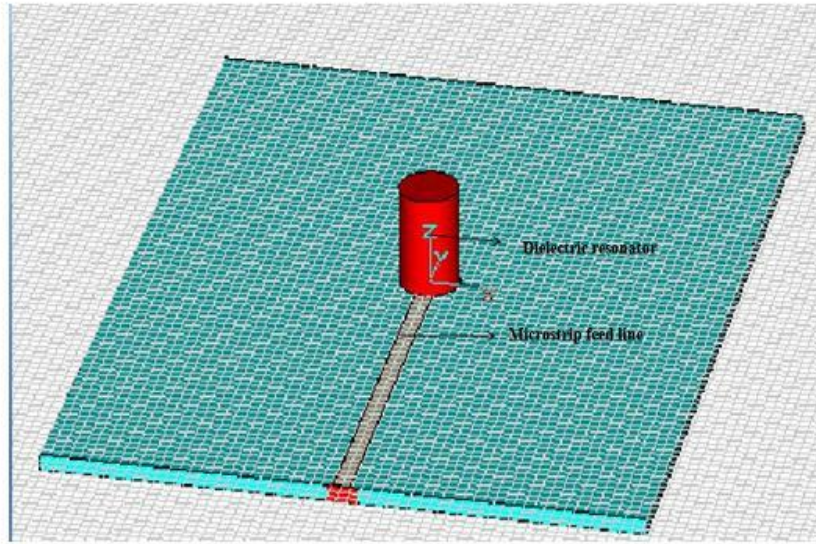


Figure 4.5 Schematic view of cylindrical DRA

As micro strip line feeding offers the advantage of easy and cost-effective fabrication of DRA, so to achieve a cost effective wideband operation the DRA is excited via micro strip line which is an effective feed mechanism to obtain wideband operation.

From the Figure 4.5 the designed cylindrical DRA has the resonant frequency at 8.93 GHz. Resonant frequencies is also theoretically calculated is 10.13 GHz using the equation (4-4).

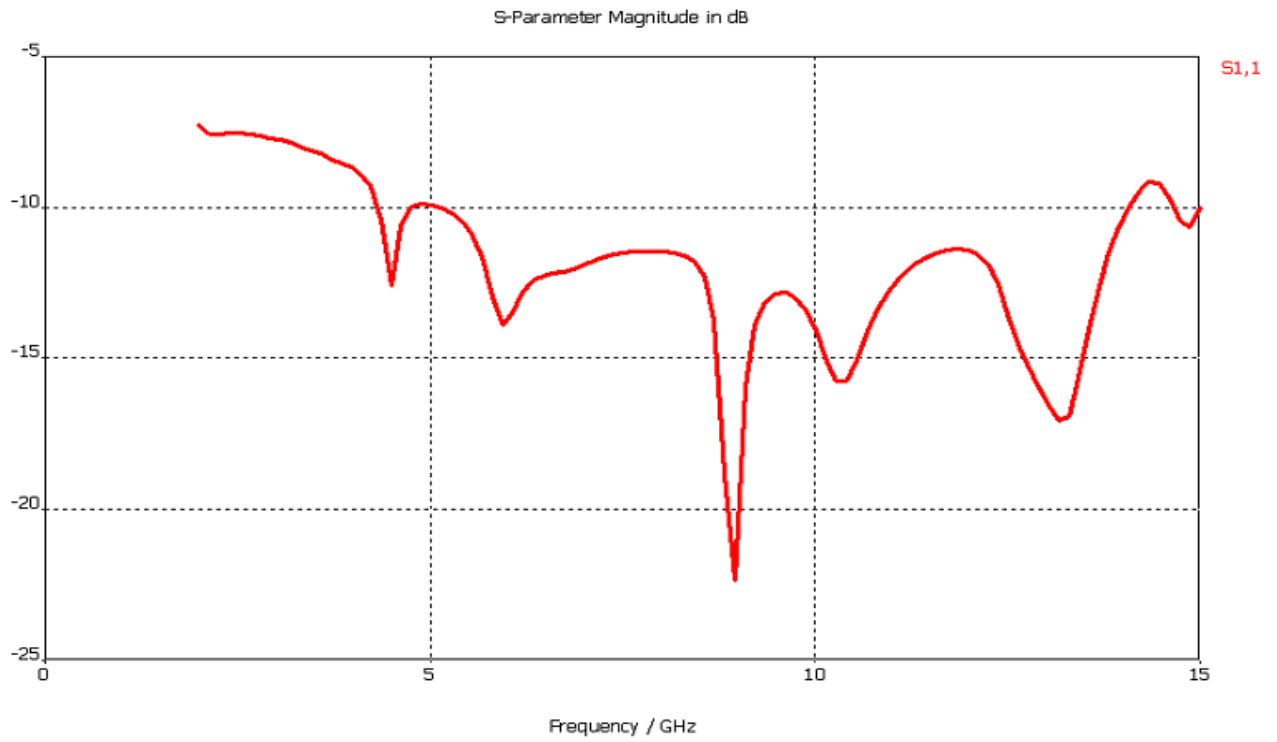


Figure 4.6 Simulated return loss versus Frequency of the cylindrical DRA

CHAPTER 5

COUPLING TO DRAs

Chapter 4 examined the basic DRAs and presented design equations for predicting the resonant frequency and radiation Q-factor for the commonly used lower order modes. The models for deriving these equations assumed the DRAs were in isolation or mounted on an infinite perfect conducting ground plane and did not account for the feeding mechanisms used to excite the DRAs. The selection of the feed and that of its location both play an important role in determining which modes are excited. This, in turn, will determine the input impedance and radiation characteristics of the DRAs. The coupling mechanism can also have a significant impact on the resonant frequency and Q-factor, which the previous equations fail to predict. This chapter begins with a brief review of coupling theory and an examination of the internal fields within rectangular and cylindrical DRAs. Knowledge of the internal field configuration is essential for understanding how the various feeds can excite different modes within the DRA. The more common feeds are then surveyed and examples provided to highlight practical design considerations.

5.1 COUPLING COEFFICIENTS

For most practical applications, power must be coupled into or out of the DRA through one or more ports. The type of port used and the location of the port with respect to the DRA will determine which mode will be excited and how much power will be coupled between the port and the antenna. The mode or modes generated, the amount of coupling, and the frequency response of the impedance

are all important in determining the performance of the DRA. Although these quantities are difficult to determine without using numerical methods, a great deal of insight can be obtained by knowing the approximate field distributions of the modes of the isolated DRA and by making use of the Lorentz Reciprocity Theorem and some coupling theory borrowed from resonator circuits [23].

When coupling to a DRA, the source can typically be modeled as either an electric or magnetic current, or the amount of coupling, χ , between the source and the fields within the DRA can be determined by applying the reciprocity theorem with the appropriate boundary conditions. For an electric source \mathbf{J}_s

$$\chi \propto (\mathbf{E}_{DRA} \cdot \mathbf{J}_s) dV \quad (5.1)$$

And for a magnetic source \mathbf{M}_s

$$\chi \propto (\mathbf{H}_{DRA} \cdot \mathbf{M}_s) dV \quad (5.2)$$

Where V is the volume occupied by the source within which the electric and/or magnetic currents exist, while E_{DRA} and H_{DRA} are the electric and magnetic fields within the DRA. Equation (5.1) states that in order to achieve strong coupling using an electric current source (like a probe), then that source should be located in an area of strong electric fields within the DRA. On the other hand, to achieve strong coupling using a magnetic current source (like a loop or an aperture) then from (5.2) the source should be located in an area of strong magnetic fields. It is thus necessary to have a good understanding of the internal field structures of the isolated DRA to determine where the feed should be placed to excite the desired mode. The fields within cylindrical and rectangular DRAs will be examined in the next section.

In addition to transferring power, the coupling mechanism to the DRA has a loading effect that will influence the Q-factor of *the* DRA. An external Q-factor (Q_{ext}) can be defined in terms of the coupling factor, χ :

$$Q_{ext} = \frac{Q}{\chi} \quad (5.3)$$

Where Q is the unloaded Q-factor. Maximum power is transferred between the coupling port and the DRA when the coupling factor is 1. This condition is known as critical coupling. When $\chi < 1$, the DRA is said to be under coupled, when $\chi > 1$ the DRA is over coupled. The more common coupling methods to DRAs will be presented later in this chapter.

5.2 FIELDS WITHIN RECTANGULAR AND CYLINDRICAL DRAS

For the rectangular DRA shown in Figure 5.1, with dimensions $w > b$ or d , the lowest order mode will be

$$E_x = 0 \quad (5.4)$$

$$E_y = k_z \cos(k_x x) \cos(k_y y) \sin(k_z z) \quad (5.5)$$

$$E_z = -k_y \cos(k_x x) \sin(k_y y) \cos(k_z z) \quad (5.6)$$

The $e^{j\omega t}$ time dependence is suppressed in the above equations.

Assuming magnetic walls along air-dielectric interfaces parallel to the z-axis, then:

$$K_y = \frac{m\pi}{w} \quad \text{and} \quad K_z = \frac{n\pi}{b} \quad (5.7)$$

For the lowest order mode ($m = n = 1$), a sketch of the field configuration is shown in Figure 5.1. The H_x component of the magnetic field is dominant along the center of the DRA, while the E-fields (predominantly E_y and E_z) circulate around the H_x component. These fields are similar to those produced by a short magnetic dipole. A plot of the relative amplitudes of the electric and magnetic fields in the x-y plane of the DRA is shown in Figure

5.2. A knowledge of the relative amplitudes of these fields as a function of location within the DRA is important for determining where to place the feed mechanism to efficiently excite the DRA.

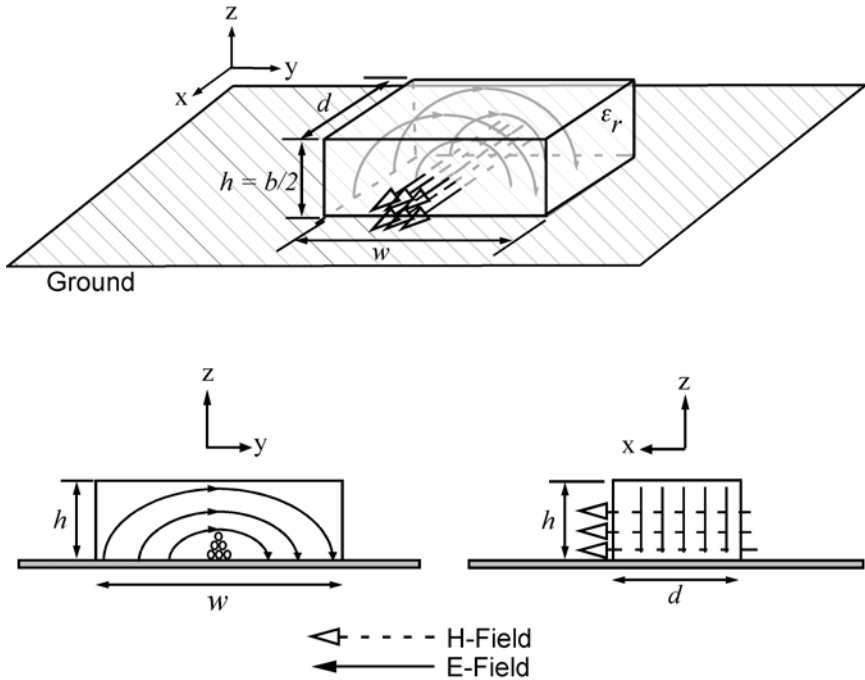


Figure 5.1 Sketch of the fields for the rectangular DRA

Higher-order modes of rectangular DRAs can also be excited for certain aspect ratios. Figure 5.2 shows sketches of the electric fields of some of these modes. The $TE_{\delta 31}^x$ and $TE_{\delta 13}^x$ modes will produce radiation patterns similar to the $TE_{\delta 31}^x$ mode, having a peak in the broadside direction (along the z-axis), while the $TE_{\delta 21}$ mode will have a null at broadside. (Note that the $TE_{\delta 12}$ mode cannot exist for the case of the DRA mounted on the ground

plane, due to the boundary condition that forces the tangential E-field to zero at $z = 0$, since the TE δ_{12} would require the E-field to be maximum at that location.) By properly combining one or more of the higher-order modes with the fundamental mode, a wider bandwidth or dual-band operation can be achieved [25].

The fields of a cylindrical DRA operating in the TE $_{01\delta}$ mode can be approximated by

$$H_z \propto J_o(\beta r) \cos \frac{\pi z}{2h} \quad (5.8)$$

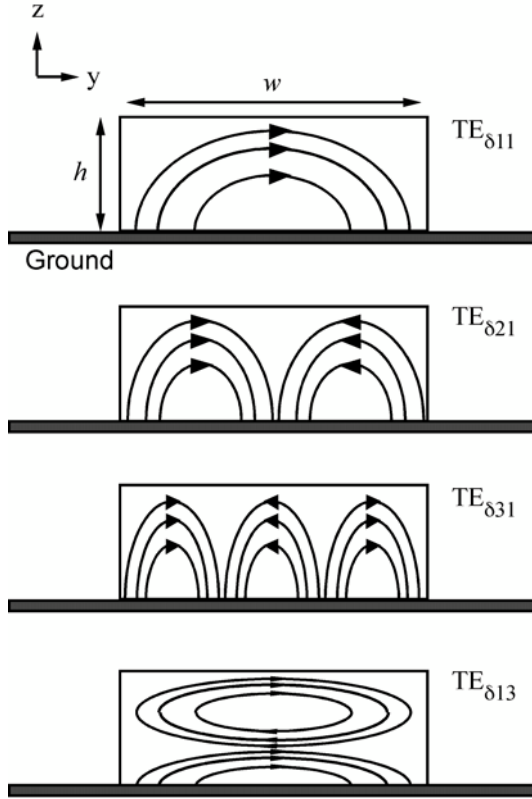


Figure 5.2 Sketches of the E-fields for selected higher-order modes within the rectangular DRA.

$$E_{\phi} \propto J_1(\beta r) \cos \frac{\pi z}{2h} \quad (5.9)$$

$$E_z = E_r = H_\phi = 0 \quad (5.10)$$

Where $J_o(\beta)$ and $J_l(\beta)$ are Bessel functions of the first kind, and β is the solution to $J_o(\beta a) = 0$.

The $TM_{01\delta}$ fields are similar to those of the $TE_{01\delta}$ with the magnetic and electric field components interchanged. The fields for these three modes are sketched in Figure 5.4. Examples of the relative field strengths for these modes are shown in Figures 5.5 and 5.6. The actual values will depend on the dielectric constant and radius of the DRAs; however, these figures are useful for visualizing the locations of high electric and magnetic fields within the DRA for the different modes, to assist in determining what type of feed is best suited and where the feed should be located to optimize the DRA excitation. The following sections will examine the more conventional coupling mechanisms in closer detail.

5.3 APERTURE COUPLING

One common method of exciting a DRA is through an aperture in the ground plane upon which the DRA is placed. Figure 5.4 shows some of the aperture shapes that have been used for exciting DRAs. The small rectangular slot is probably the most widely used aperture [26-27]. By keeping the slot dimensions electrically small, the amount of radiation spilling beneath the ground plane can be minimized. Annular slots have also been used for exciting cylindrical

DRA's , while cross-shaped and C-shaped slots are used to excite circular polarization [28-29]. The aperture can itself be fed by a transmission line (either micro strip or coaxial) or a waveguide as shown in Figure 5.4. Aperture coupling offers the advantage of having the feed network located below the ground plane, isolating the radiating aperture from any unwanted coupling or spurious radiation from the feed.

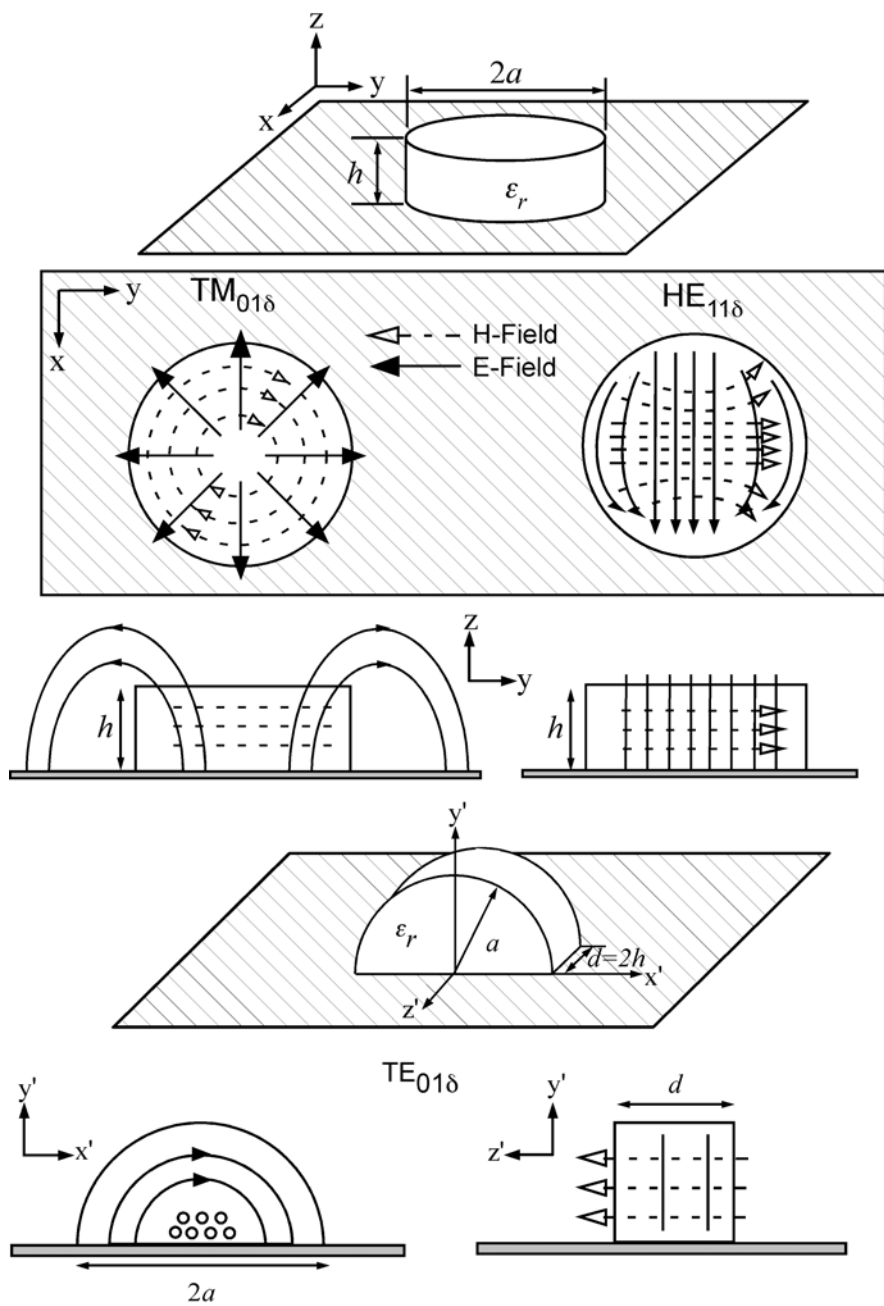


Figure 5.3 Sketch of the cylindrical DRA field configurations.

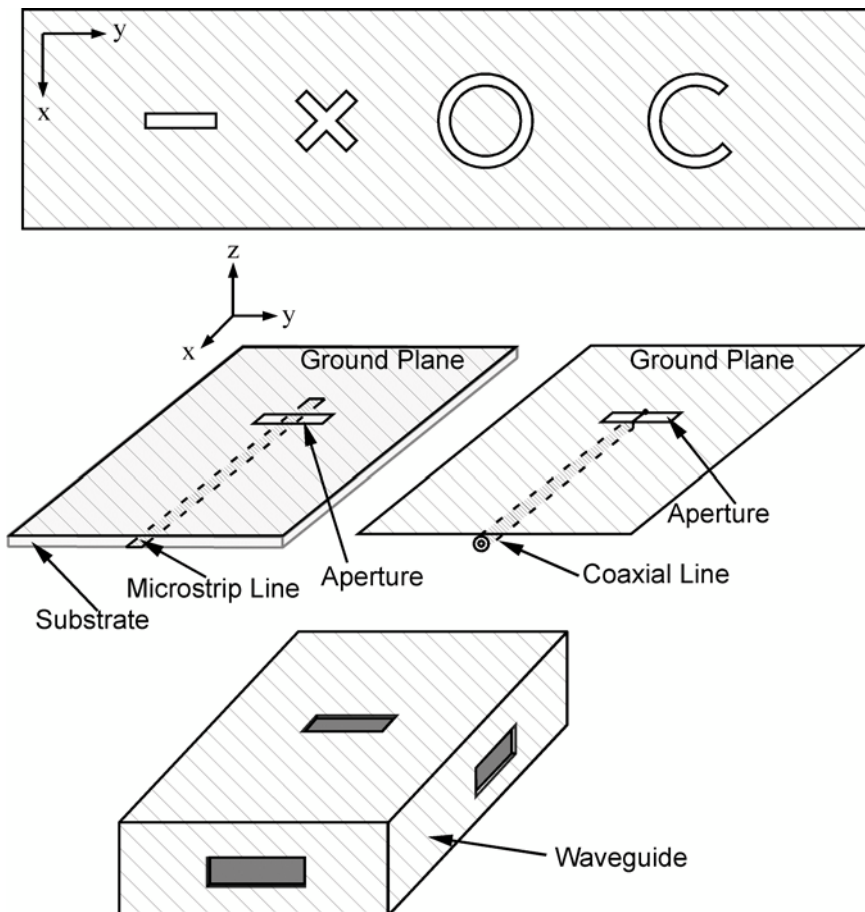


Figure 5.4 Various slot apertures.

The electric fields within a rectangular slot are sketched in Figure 5.5. For coupling purposes, the slot can be considered as an equivalent magnetic current whose direction is parallel to the slot length. To achieve strong coupling to the DRA, the aperture should be located in a region of strong magnetic fields, as indicated by (5.2).

Figure 5.6 shows a rectangular slot feeding a rectangular DRA.

The orientation of the slot will excite the $TE_{\delta 11}^x$ mode of the DRA . Centering the DRA over the slot will ensure strong coupling to the internal magnetic fields. Some degree of impedance matching can be achieved by offsetting the DRA from the slot center. A rectangular slot can also be used to excite the $HE_{11\delta}$ mode of a cylindrical DRA or the $TE_{01\delta}$ mode of a split-cylinder DRA, as shown in Figures 5.7 and 5.8 .

Feeding the aperture with a micro strip transmission line is the most common approach, since printed technology is easy to fabricate. Micro strip lines also offer a

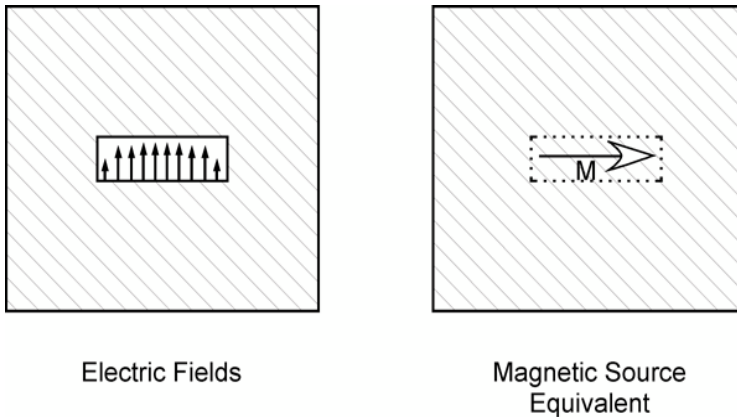


Figure 5.5 Equivalent magnetic current for slot apertures.

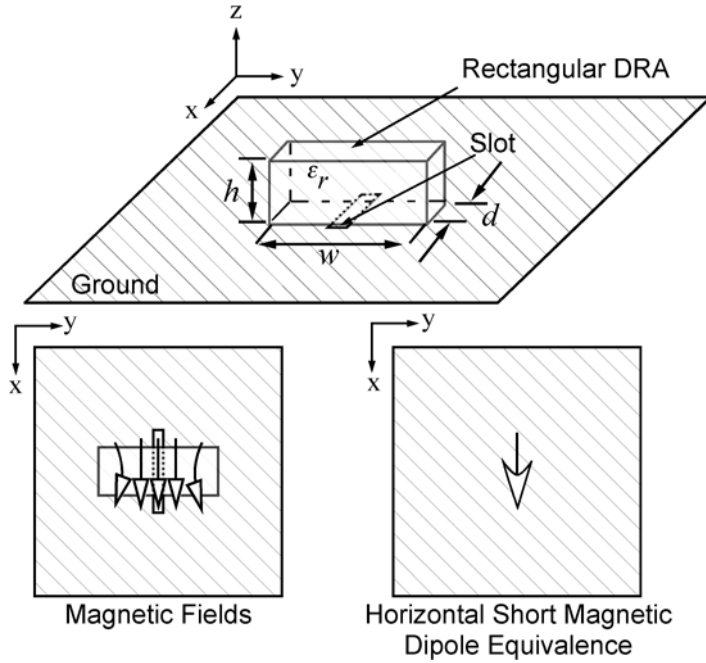


Figure 5.6 Slot apertures coupling to a rectangular DRA.

degree of impedance matching not available with coaxial lines or waveguides. As shown in Figure 5.9, the micro strip line can be extended by a distance s beyond the slot. This extension behaves like an open-circuit stub, whose admittance is in parallel with the admittance of the slot. By adjusting the length s of the stub, the reactive component of the slot admittance can be reduced (and, in theory, completely cancelled at the design frequency), resulting in an improved impedance match to the micro strip line. The techniques for aperture coupling to DRAs are similar to those of a micro strip patch antenna, and as a rule of thumb, the stub length is chosen to be $s = \lambda_g/4$, where λ_g is the guided wavelength of the micro strip line. The

slot length l_s and width w_s will control the amount of coupling from the micro strip line to the DRA. The area of the slot should, in general, be kept as small as possible to avoid excessive radiation beneath the ground plane. Also, if the aperture is too large, it will significantly load the DRA, and the resonant frequency will shift compared to the theoretical value obtained using the models. The aperture introduces an air gap beneath the DRA, which will then no longer see a continuous ground plane. If the aperture is too large, the previous assumptions using image theory to double the height of the DRA become less accurate, resulting in larger errors in the predicted resonant frequency and Q-factor.

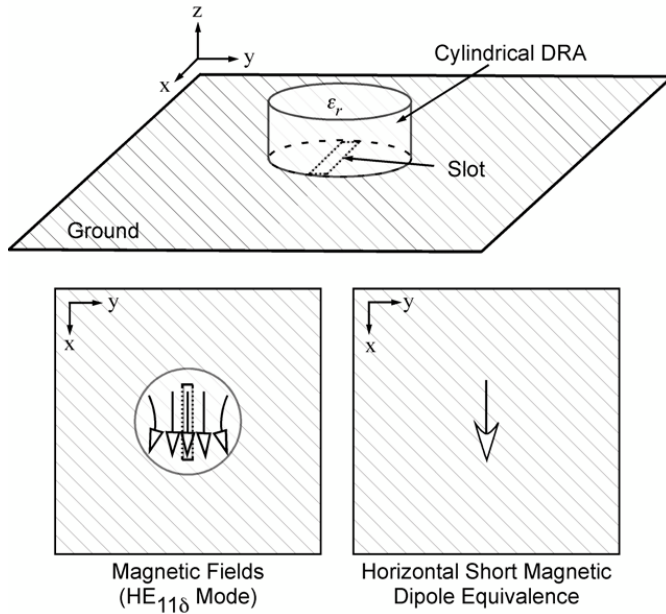


Figure 5.7 Slot apertures coupling to a cylindrical DRA.

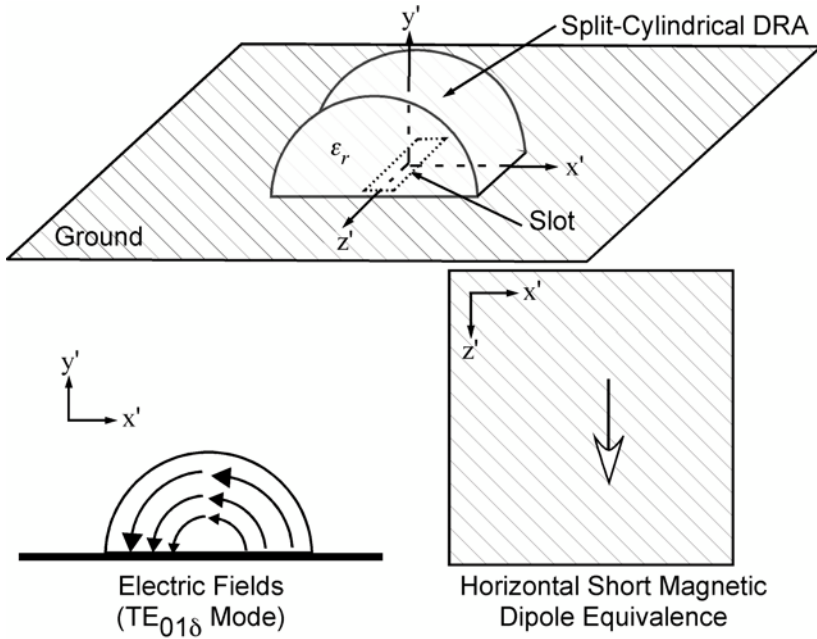


Figure 5.8 Slot apertures coupling to a split-cylindrical DRA.

Computational electromagnetic methods, such as the finite element method, the method of moments, or the finite-difference time domain method are typically used to determine the input impedance of slot-fed DRAs. Several commercial software packages are available for analyzing three-dimensional electromagnetic problems, which can be used to predict the input impedance with a reasonably high degree of accuracy. These software tools are better suited for analysis than design, since the computational time can be lengthy, especially for high values of the dielectric constant. Although there are no simple equations for designing the slot dimensions given the various antenna parameters, the following guidelines can be used as a starting point for rectangular slots:

- 1) The slot length l_s is chosen large enough so that sufficient coupling exists between the DRA and the feed line but small enough so that it does not resonate within the band of operation, which usually leads to a significant radiated back lobe.

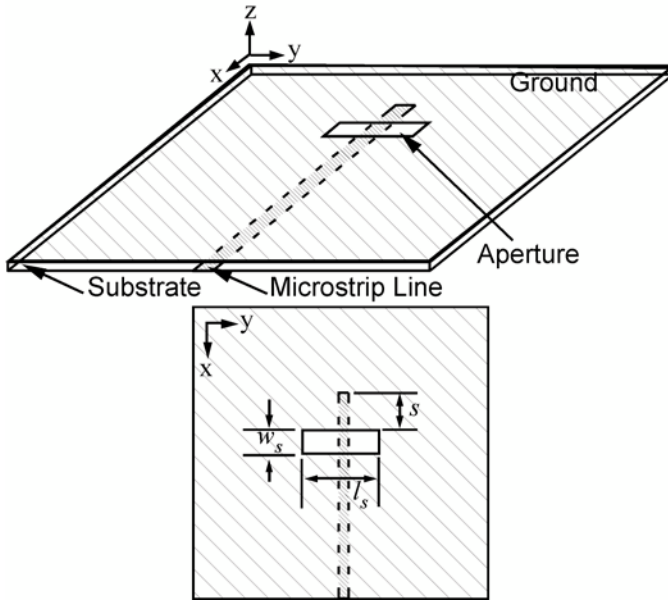


Figure 5.9 Micro strip-fed rectangular slots.

Where

$$\epsilon_e = \frac{\epsilon_r + \epsilon_s}{2} \quad (5.10)$$

and ϵ_r and ϵ_s are the dielectric constants of the DRA and substrate, respectively.

- 2) A fairly narrow slot width is usually chosen to avoid a large back lobe component. A reasonable choice is:

$$w_s = 0.2l_s \quad (5.11)$$

At high frequencies, (5.11) might result in a very narrow slot that may be difficult to fabricate due to etching limitations. At these frequencies, a wider slot width can be used.

- 3) The stub extension s is selected so that its reactance cancels out that of the slot aperture. It is generally initially chosen to be:

$$s = \frac{\lambda_g}{4} \quad (5.12)$$

Where λ_g is the guided wave in the substrate.

The amount of coupling actually achieved using the above guidelines is not always as high as desired. Oftentimes the coupling can be significantly improved simply by slightly offsetting the DRA with respect to the slot. This solution requires neither a second design iteration nor the fabrication of a new circuit and is an attractive method for obtaining a good impedance match [24].

5.4 PROBE COUPLING

Another common method for coupling to DRAs is with a probe, as shown in Figure 5.10 [30-31]. The probe usually consists of the center pin of a coaxial transmission line that extends through the ground plane. The center pin can also be soldered to a flat metal strip, that is placed adjacent to the DRA, whose length and width can be adjusted to improve the impedance match. Instead of a coaxial line, the flat metal strip can also be connected to a micro strip line . For coupling purposes, the probe can be considered as a vertical electric current, as shown in Figure 5.10 and, from (5.1), it should be located in a region of the DRA having high electric fields to achieve strong coupling. The probe can either be

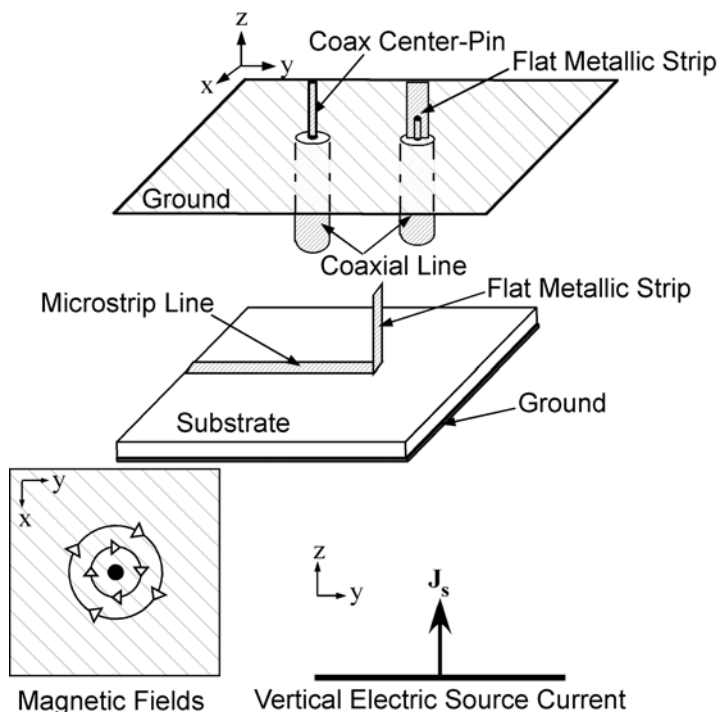


Figure 5.10 Vertical probe sources.

located adjacent to the DRA or can be embedded within it. The amount of coupling can be optimized by adjusting the probe height and the DRA location. Also, depending on the location of the probe, various modes can be excited.

A probe located adjacent to (or slightly inset into) a rectangular DRA, as shown in following figure and cylindrical DRA or the $TE_{01\delta}$ mode of the split cylinder can be excited with a probe located adjacent to (or slightly inset into) the DRA, as in Figures 5.12 and 5.13. For a probe located in the center of a cylindrical (or ring) DRA, the $TM_{01\delta}$ mode is excited, as shown in Figure 5.14. One advantage of coaxial probe excitation is the direct

coupling into a $50\text{-}\Omega$ system without the need for a matching network. Probes are useful at lower frequencies where aperture-coupling may not be practical due to the large size of the slot required.

The probe length is generally chosen to be less than the height of the DRA, to avoid probe radiation. Rigorous analyses for probe-fed hemispherical and cylindrical DRAs have been carried out, showing the effects of both the probe position and length on the input impedance and resonant frequency

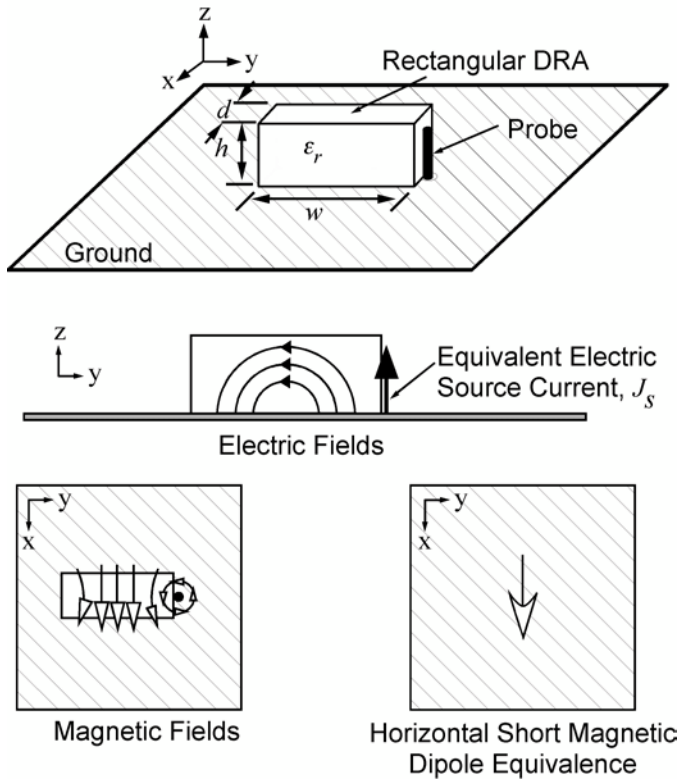


Figure 5.11 Probe coupling to a rectangular DRA.

of the DRA [32]; however, there are no simple equations to design the required probe height for a given set of DRA dimensions and dielectric constant. In terms of practicality, locating the probe feed adjacent to the DRA is preferred since it does not require drilling into the DRA. (This, of course, cannot be avoided for the $TM_{01\delta}$ mode of cylindrical DRAs where the probe must be at the center of the DRA.) If the center conductor of a coaxial cable is used as the probe, one approach is to begin with a probe height slightly taller than that of the DRA, then trimming the height until the desired match is achieved. Similarly, if a flat metallic strip is used, it is recommended to start with a taller, wider strip which can be then trimmed for impedance tuning.

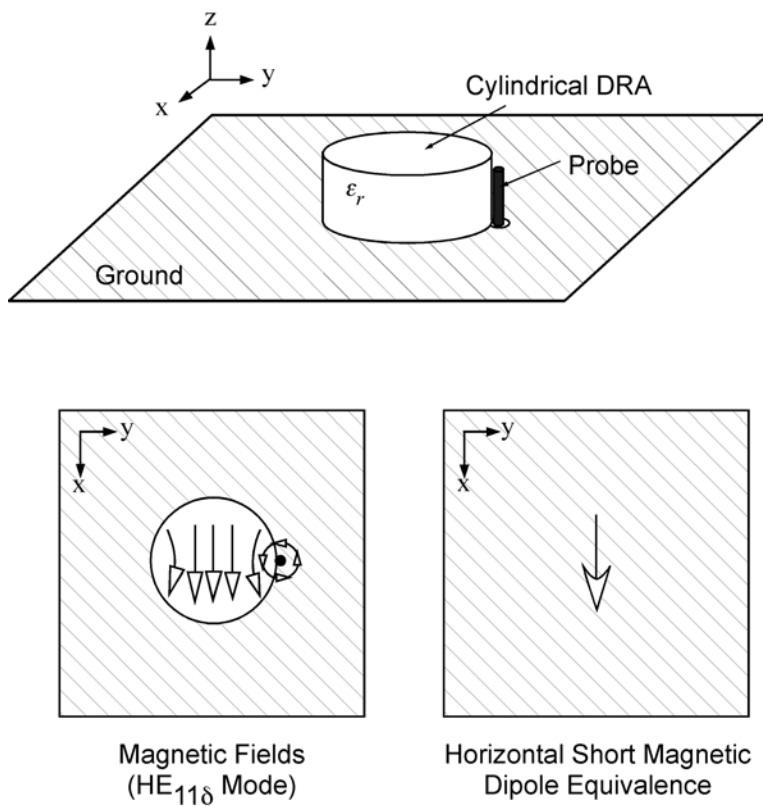


Figure 5.12 Probe coupling to the $HE_{11\delta}$ mode of the cylindrical DRA.

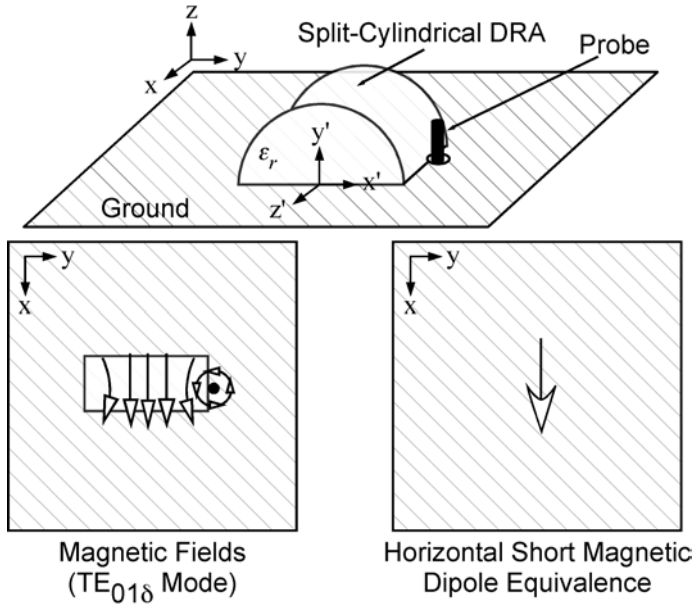


Figure 5.13 Probe coupling to split-cylindrical DRAs.

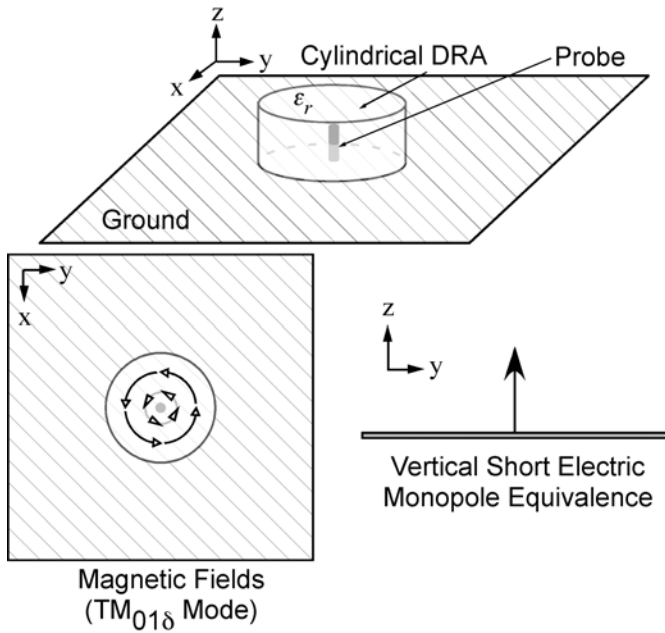


Figure 5.14 Probe coupling to the $TM_{01\delta}$ mode of the cylindrical DRA.

5.5 MICROSTRIP LINE COUPLING

A common method for coupling to dielectric resonators in microwave circuits is by proximity coupling to micro strip lines. Figure 5.15 shows this feeding technique applied to DRAs [33]. Micro strip coupling can be used to excite the $TE_{\delta 11}^x$ mode of the rectangular DRA or the $HE_{11\delta}^x$ mode of cylindrical DRA as shown in fig. This sketches the magnetic fields in the DRA and the equivalent short horizontal magnetic dipole mode.

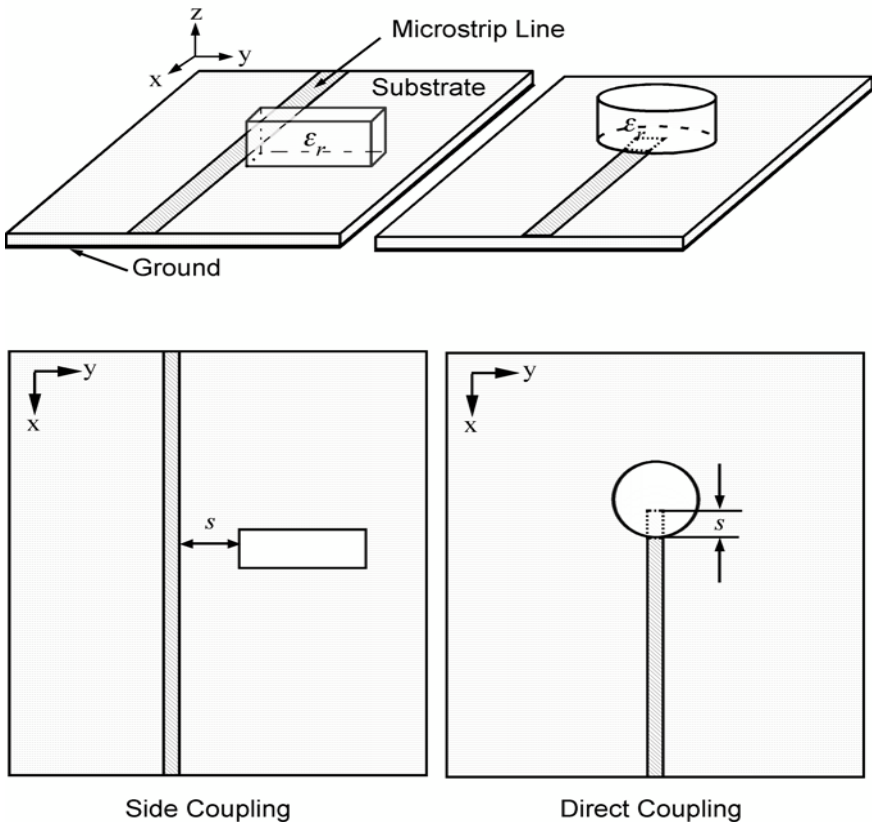


Figure 5.15 Micro strip line coupling to DRAs.

The amount of coupling from the micro strip line to the DRA can be controlled to a certain degree by adjusting s in Figure 5.15, which represents the spacing between the DRA and the line for the side-coupled case or the length of the line underneath the DRA for the direct-coupled case. A more dominant parameter affecting the degree of coupling is the dielectric constant of the DRA. For higher values ($\epsilon_r > 20$), strong coupling is achieved; however, the maximum amount of coupling is significantly reduced if the dielectric constant of the DRA is lowered. This can be problematic if low dielectric constant values are required for obtaining wideband operation. For series-fed linear arrays of DRAs, the lower level of coupling may not be an impediment, since each DRA element usually only requires coupling a small amount from the micro strip feed line [34].

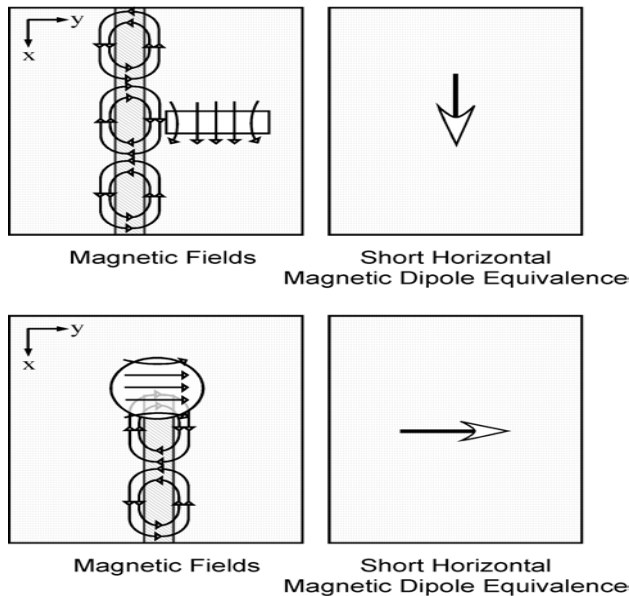


Figure 5.16 Fields and equivalent radiation models of micro strip line-coupled DRA

5.6 COPLANAR COUPLING

Coupling to DRAs can also be achieved by using coplanar feeds with some examples shown in Figure 5.17 [35]. Open-circuit coplanar waveguides can be used to directly feed DRAs similar to the open-circuit micro strip lines examined earlier. Additional control for impedance matching can be achieved by adding stubs or loops at the end of the line. Figure 5.18 shows a cylindrical DRA coupled to a coplanar loop. The coupling level can be adjusted by positioning the DRA over the loop. The coupling behavior of the coplanar loop is similar to that of the coaxial probe, but the loop offers the advantage of being non obtrusive. By moving the loop from the edge of the DRA to the center, one can couple into either the $HE_{11\delta}$ mode or the $TE_{01\delta}$ mode of the cylindrical DRA [35]. As with aperture coupling, the dimensions of the coplanar feed should be chosen large enough to ensure proper coupling, but small enough to avoid excessive radiation in the back lobe.

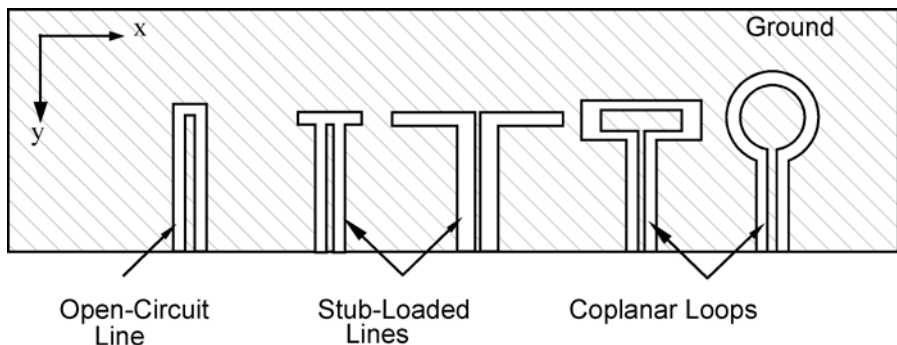


Figure 5.17 Various coplanar feeds for coupling to DRAs.

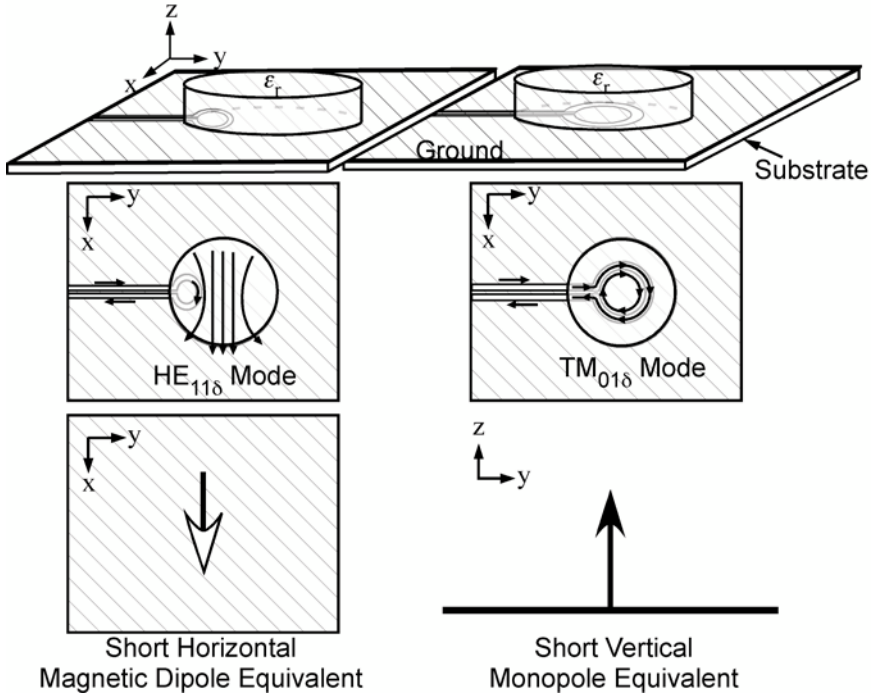


Figure 5.18 coplanar loops coupling to a cylindrical DRA.

5.7 DIELECTRIC IMAGE GUIDE COUPLING

The final method of coupling to DRAs presented in this chapter is by way of a dielectric image guide, as shown in Figure 5.19. Dielectric image guides offer advantages over micro strips at millimeter-wave frequencies, since they do not suffer as severely from conductor losses. As with micro strip lines, the amount of coupling to the DRA is generally quite small, especially for DRAs with lower

dielectric constants, although it may be possible to increase the coupling by operating the guide closer to the cut-off frequency. The dielectric image guide is thus best utilized as a series feed to a linear array of DRAs.

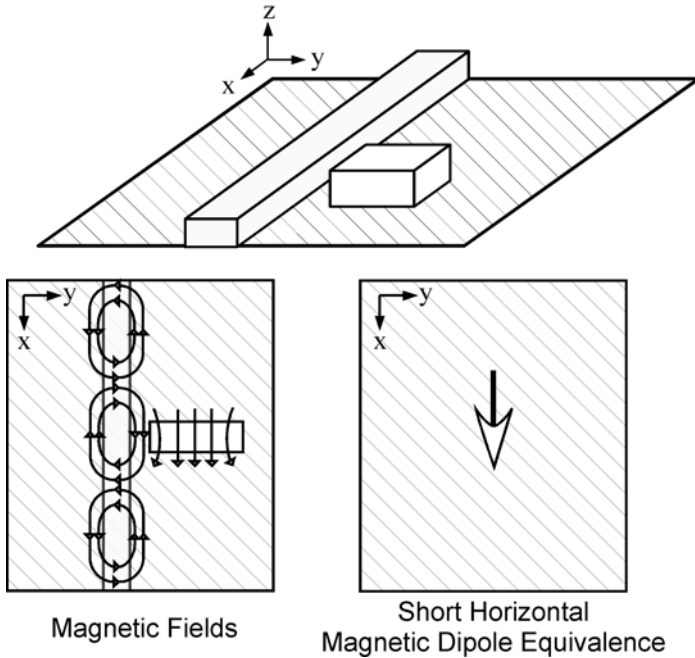


Figure 5.19 Dielectric image guide feed for DRAs.

5.8 SURVEY OF ANALYTICAL METHODS

One important parameter in designing a feed to excite the DRA is the input impedance. Knowledge of the input impedance as a function of frequency is needed to determine the bandwidth of operation and for matching the antenna to the circuit. In this chapter, guidelines were given for the various coupling mechanisms to help

obtain a good impedance match that did not rely on knowledge of the DRA input impedance. These guidelines offer a good starting point for the design, but do not allow for precise designs if specific impedances are required. Unfortunately, there are no simple closed-form expressions for predicting the input impedance of the DRA when excited by a particular feed and rigorous analytical or numerical techniques are required. This section provides a brief survey of some of the techniques that have been used to predict the input impedance for DRAs excited by the various feeds.

5.8.1 Frequency Domain Analysis

Two common frequency domain techniques that have been used to analyze DRAs are the method of moments (MOM) and the finite element method (FEM). The MOM involves discretizing the antenna into a number of small segments and solving for a set of unknown coefficients, each coefficient representing the current on one segment due to a known incident field [36]. Once the currents are determined, the input impedance of the antenna can then be calculated. The MOM was first developed for wire or metal antennas of arbitrary shape, but can be extended to include dielectric materials by introducing equivalent currents. By using the MOM, analysis of DRAs is not limited to a hemispherical shape, and the technique can be used to also analyze simple cylindrical and rectangular DRA shapes [36]. Determining the DRA input impedance using the MOM technique will

require more computer memory and time than applying Green's function, since the DRA must usually be finely segmented to obtain an accurate solution (especially when they are made of high dielectric constants). The MOM technique is therefore not as convenient a tool for optimizing the DRA performance.

The FEM is a second frequency domain technique and can be used to analyze DRAs of arbitrary shape. Similar to the MOM, it involves a discretization of the geometry (usually using small tetrahedrons), but whereas in the MOM only the DRA and the ground plane require segmentation, in the FEM technique, the entire volume surrounding the DRA must also be discretized, thereby increasing the computational size of the problem. The advantage of the FEM is that it does not require the formulation of equivalent currents and can thus be readily applied to arbitrary shapes. Another advantage of the FEM is its availability as commercial software where graphical user interfaces are provided to simplify the geometrical definition of the problem. Examples of the use of the FEM to analyze DRAs can be found in . The FEM is used to determine the effects of a finite ground plane on the radiation patterns of a DRA.

5.8.2 Time Domain Analysis Techniques

Two time domain techniques that have been applied to analyzing DRAs are the finite difference time domain (FDTD) method and the transmission line method (TLM). Just as with the FEM, these time domain techniques require the entire volume around the DRA to be

discretized and thus can be memory and time intensive. For the FDTD and TLM methods, small cubes are used for discretization, instead of tetrahedrons, and care must be taken to properly model curved geometries, due to the stair-stepping effect. Time domain techniques use a wideband pulse to excite the DRA, and by transforming the solution into the frequency domain, the input impedance can be determined over a wide frequency range. For the frequency domain techniques, the problem would have to be re-simulated at every frequency of interest and obtaining the impedance response over a broad frequency range could be very time consuming. Commercial software has also been developed for the FDTD and TLM techniques, eliminating the necessity for designers to develop their own codes. Examples of DRAs analyzed using time domain methods can be found in [10]. Again, as with the frequency domain methods, the time domain methods are good tools for analyzing the performance of a given DRA geometry, but are less useful for optimizing the performance of DRAs. However, with the continual increase in the speed and memory of computers, it may not be long before these methods can also serve as optimization tools, providing solutions within reasonable times.

CHAPTER 6

ANTENNA DESIGN AND MEASUREMENT RESULTS

6.1. INTRODUCTION

The world of Ultra-wideband (UWB) has developed dramatically in very recent years, UWB antenna is one of the critical component in the UWB system. Ideally, the performance of a UWB antenna needs to be uniform and consistent over the entire operating band. In general, aside from attaining a sufficient impedance bandwidth, high efficiency, small size, and consistent radiation pattern are required for UWB antenna. These days, a lot of flat type UWB antenna were proposed due to small size and easily embedded into wireless devices and microwave circuits. For many of the existing and emerging communication applications, wide-band antenna operation is desirable to accommodate the increasing data rates required for services such as video conferencing, direct digital broadcast, EHF portable satellite communications, local multi-point communications, and indoor wireless. Some of these requirements may be met by existing printed antenna technology, but with the added cost and complexity associated with multi-layer configurations required for achieving broad bandwidths. This section presents some novel DRAs of relatively simple design, which have demonstrated wide-band performance, and may serve as suitable antenna candidates for these various applications.

There are a number of definitions describing antennas operating in the millimeter-wave (MMW) bands. Most commonly, antennas operating in frequencies whose wavelengths are measured in millimeters (30 GHz–300 GHz) are referred to as millimeter wave antennas. As mentioned previously, challenges associated with antennas at high frequencies include fabrication tolerances, efficiency/losses, and cost, though these are all somewhat inter-related. As is often the case, it can be very difficult to optimize each of these parameters simultaneously, and a number of approaches have already been pursued and developed. In this section, we discuss technologies used for the fabrication of different MMW antennas. We discuss these under the categories of (1) waveguide antennas, (2) printed planar antennas, and (3) on-chip antennas, which may be fabricated using micromachining or semiconductor lithography techniques referred to as W-band or the 94 GHz band) is also governed by the FCC Part 15 regulations for unlicensed operation, though for indoor applications only. The 94 GHz band may also be used for licensed outdoor applications for point-to-point In the 1990's, the advent of automotive collision avoidance radar at 77 GHz marked the first consumer-oriented use of millimeter wave frequencies above 40 GHz. In 1995, the FCC (US Federal Communications in the US, four bands in the upper millimeter wave region have been opened for commercial applications. Of the four bands, the 59-64 GHz band (commonly referred to as V-band or the 60GHz band) is governed by FCC Part 15 for

unlicensed operations. The regulations of FCC Part 15 and the significant absorption of the 60 GHz band by atmospheric oxygen makes this band better suited for very short range point-to-point and point-to-multipoint applications. The 92GHz-95GHz band (commonly wireless communication per FCC Part 101 regulations. However the band is less spectrally efficient than the other three bands due to an excluded band at 94-94.1 GHz.

In the past few years, the interest in the millimeter-wave spectrum at 30 to 300 GHz has drastically increased. The emergence of low cost high performance CMOS technology and low loss, low cost organic packaging material has opened a new perspective for system designers and service providers because it enables the development of millimeter-wave radio at the same cost structure of radios operating in the gigahertz range or less. In combination with available ultra-wide bandwidths, this makes the millimeter-wave spectrum more attractive than ever before for supporting a new class of systems and applications ranging from ultra-high speed data transmission, video distribution, portable radar, sensing, detection and imaging of all kinds. This section presents some novel DRAs of relatively simple design, which have demonstrated millimeter band performance, and may serve as suitable antenna candidates for these various applications.

6.2 Design and Analysis of I-shape dielectric resonator antenna

The increasing use of microwave mobile communication systems demand the antennas for different systems and standards with properties like reduced size, broadband, multiband operation, moderate gain etc. the planar and dielectric resonator antennas are the present day antenna designer's choice. The design of proposed antenna has been mentioned below. In the design a DR material has been chosen $\epsilon_r=10.2$ (Rogers RO3010) of size $l_1=10$ mm, $w_1=0.9$ mm, $h_1=2$ mm. There is another strip whose dimensions are taken 2mm, 3.5mm, 2mm respectively. The substrate size has been considered 14mm length, 11mm width, 1.6mm height, and then the ground plane is 10mm length, 11mm width, 0.5mm height. Substrate is chosen called Teflon of dielectric value ϵ_r 2.2. The DR material of I shaped has been placed on the Teflon substrate. The above said antenna is shown in the following figure 6.6. A simple micro strip line feeding of novel design has been used to feed the antenna.

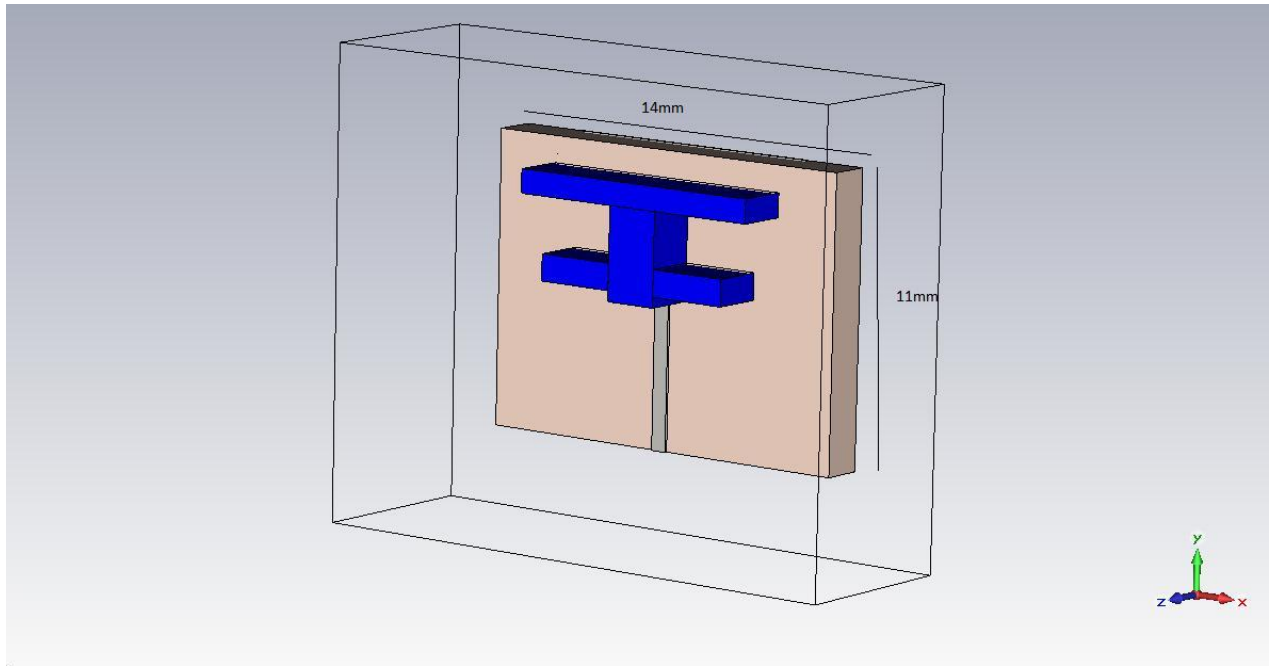


Figure 6.1 Geometry of the proposed I-shape DRA.

6.3 Simulation results and discussions

6.3.1 Reflection coefficient (S₁₁)

The proposed antenna is simulated and a return loss of -10db below is obtained which is in the range of 30.58 GHz to 39 GHz. Here a good return loss is obtained at two peaks whose values are -21db at 31.54 GHz and a value of -22db at 35.39 GHz. In this design a bandwidth improvement of 24.36% has been achieved. In addition to that a total efficiency of 72.88% is found at 35.39 GHz and 69% is found at 31.54 GHz. The design has been carried out using CST (computer simulation technology) software 2010. Here by varying the height of patch for coupling the resonant frequency is also varying.

The designed antenna is proposed for applications in the area of satellite communications, radio location, and imaging systems for weapon and hazardous material detection. This design is intended for „ka“ band (26.5-40 GHz). In satellite communications, the ka-band allows higher bandwidth communication. It is far more susceptible to signal attenuation under rainy conditions. This design is particularly meant for satellite UPLINK frequencies (31 GHz). Uplink is the portion of a communications link used for the transmission of signals from an earth terminal to a satellite (or) to an “airborne platform”. The simulated return loss of the proposed I-shape DRA plotted against frequency is shown in Fig.6.7.

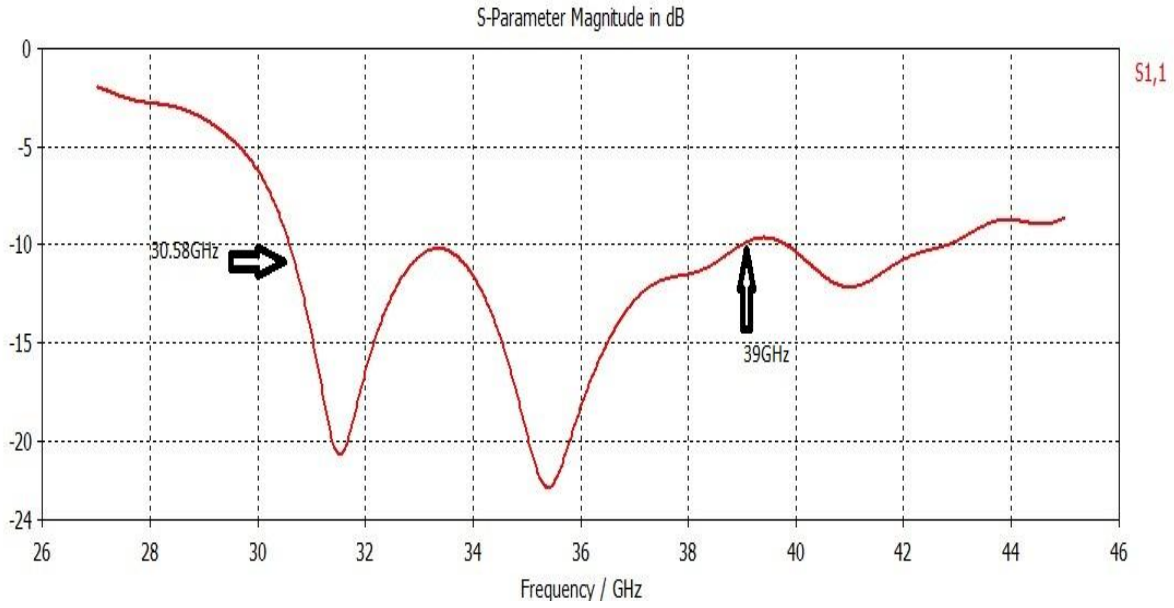


Figure 6.2 Simulated reflection coefficient (Return Loss) for the proposed I-shape DRA versus Frequency.

6.3.2 Voltage standing wave ratio

The voltage standing wave ratio (VSWR) is a well-known indication of how good the impedance match is. The VSWR is often abbreviated as SWR. A high VSWR is an indication that the signal is reflected prior to being radiated by the antenna. VSWR and reflected power are different ways of measuring and expressing the same thing.

Figure 6.8 shows the simulated voltage standing wave ratio (VSWR) for the proposed antenna. We observed that VSWR of the proposed antenna is below 2 in entire frequency range 30.58 GHz to 39 GHz.

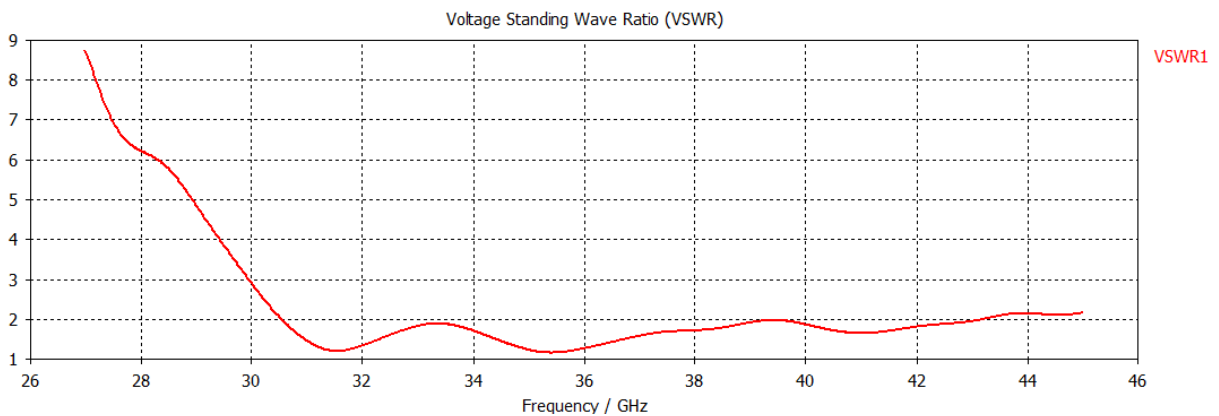


Figure 6.3 Simulated VSWR for the proposed antenna

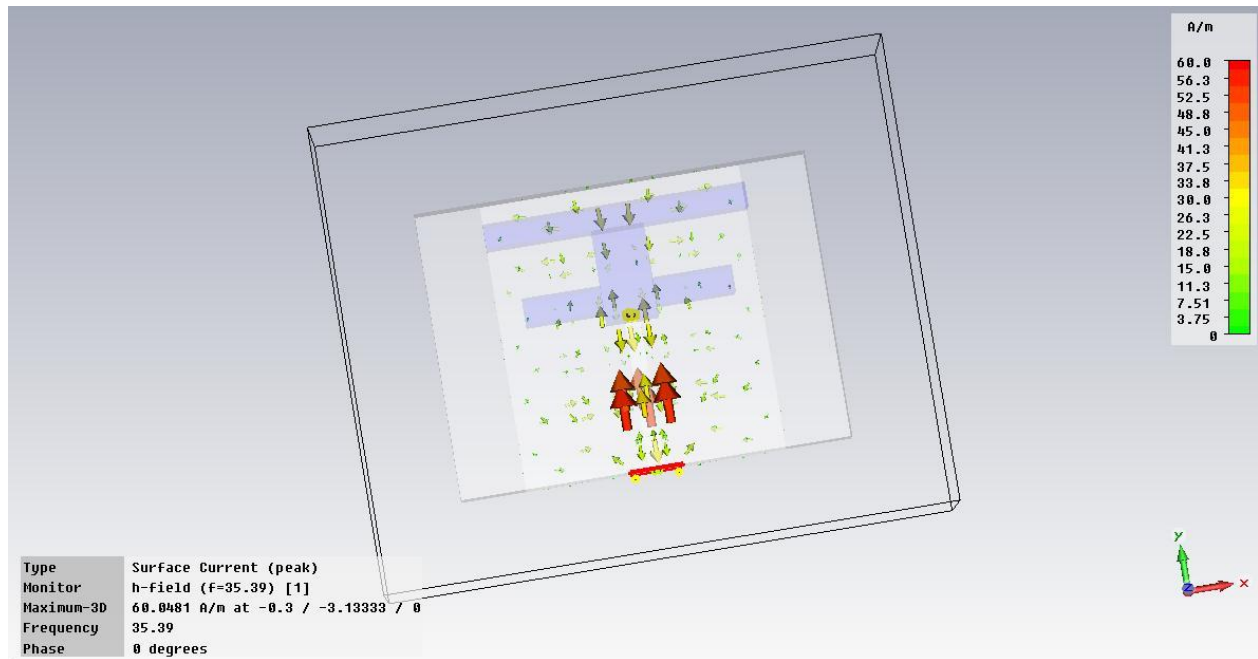


Figure 6.4 surface current flow of the proposed antenna at frequency 35.39GHz

6.3.3 Radiation directivity, gain patterns

The Peak Gain of antenna is 10.9 dBi at 35.39 GHz. It is observed from Fig. 6.10(a), (b) that the simulated peak directivity is 10.2 dBi at 35.39 GHz frequency range. In addition to that a total efficiency of 72.88% is found at 35.39 GHz and 69% is found at 31.54 GHz.

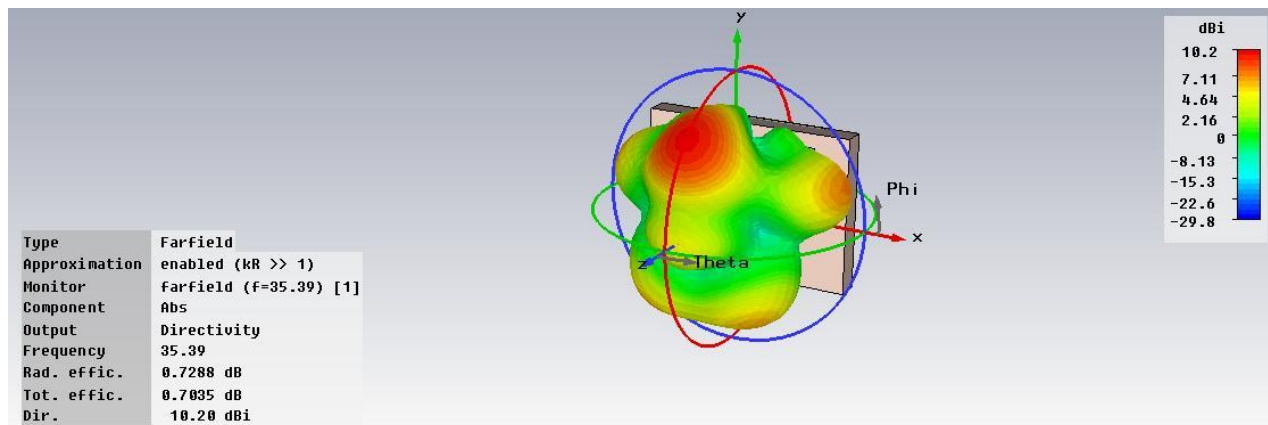


Figure 6.5 3-D view radiation pattern of the directivity of proposed DRA at frequency 35.39GHz

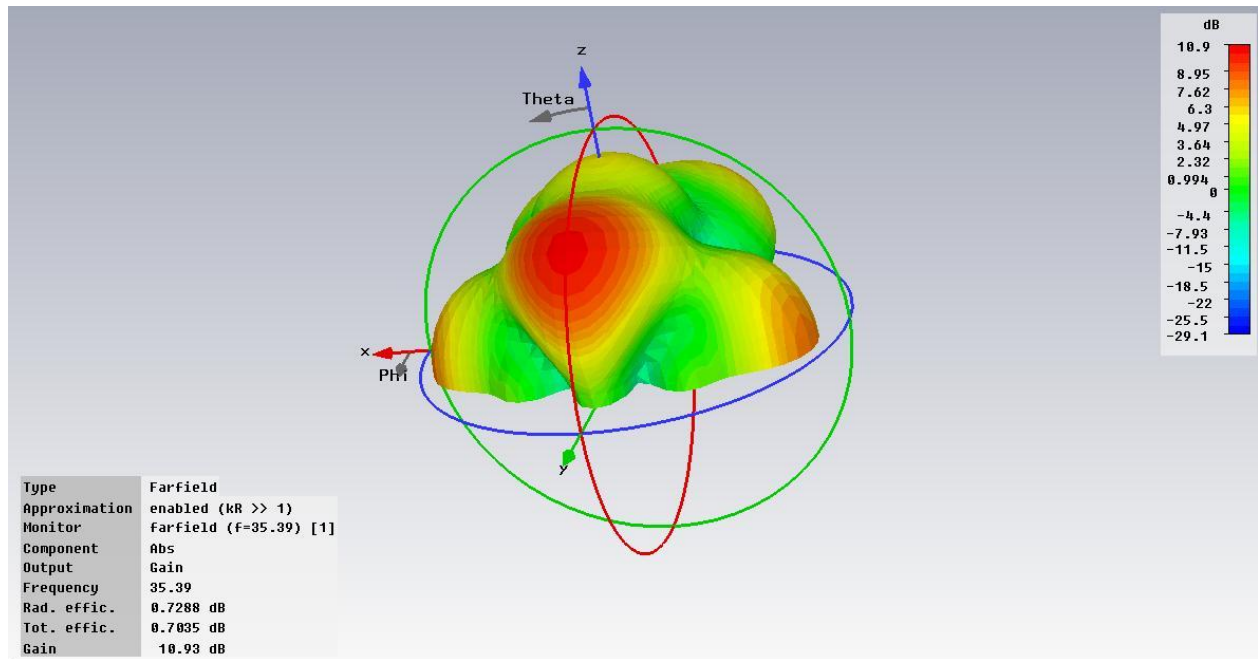


Figure 6.6 3-D view radiation pattern of the Gain of proposed DRA at frequency 35.39GHz.

6.4 Design of UWB antenna

This antenna is designed to cover the maximum portion of the UWB range. In this design a Teflon material of dielectric constant 2.1 has been used and the dielectric constant value of the substrate material is 4.4(FR4). The design has been placed on a partial ground. The design has been shown in the following figure

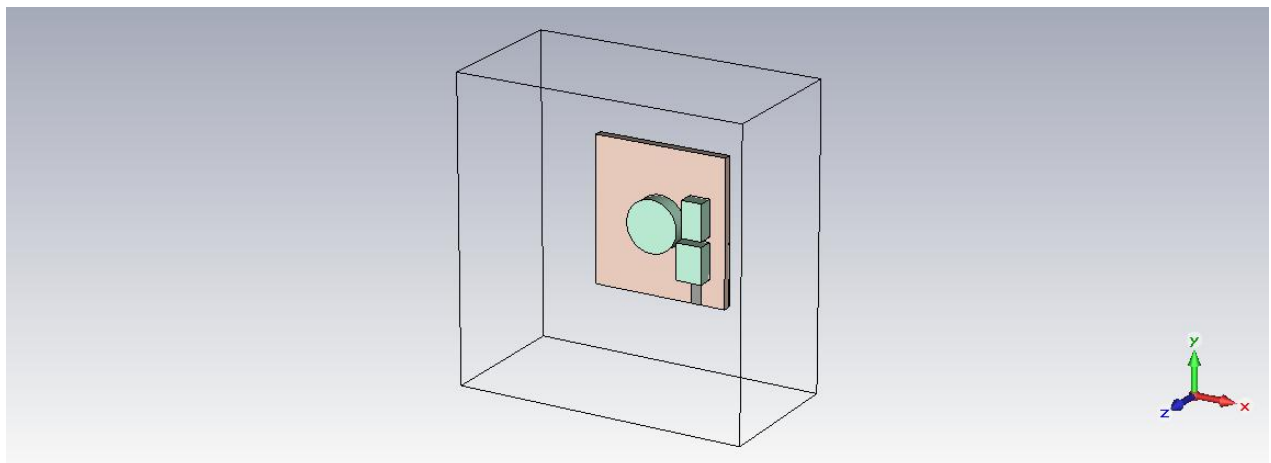


Figure 6.7 Design of UWB antenna

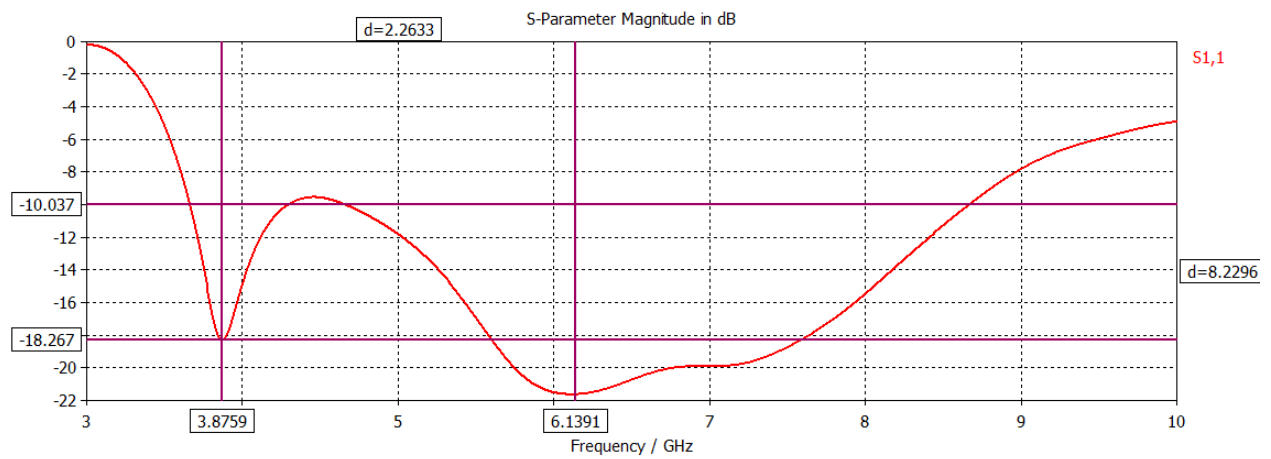


Figure 6.8 Return loss graph of the antenna

The return loss shows that a maximum value -22dB has been noticed at 6.13 GHz and a moderate value of -18.26dB is noticed at 3.875GHz

The following figure will show the measured values of return loss antenna design.

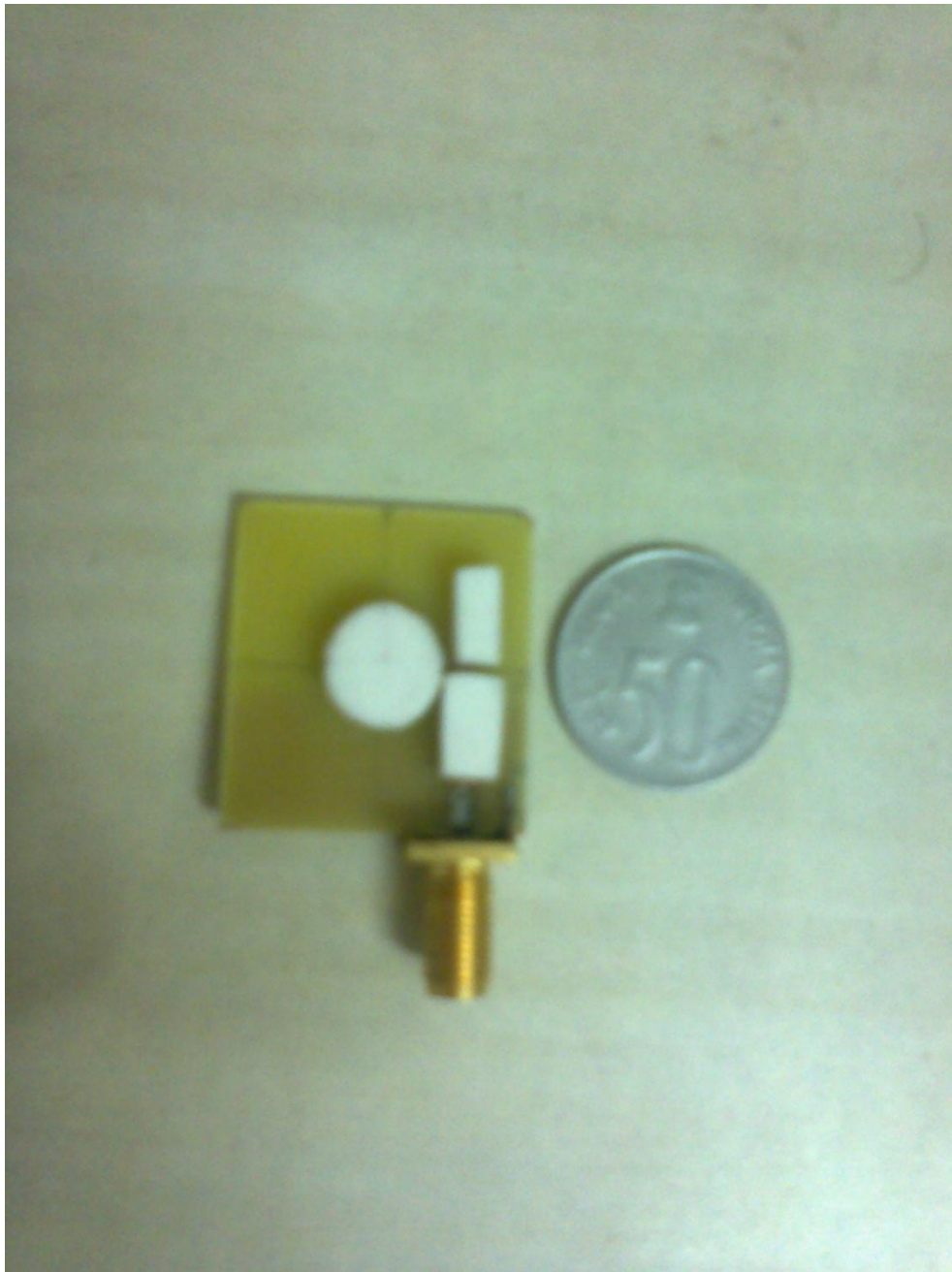


Figure 6.9 Fabricated DR antenna for UWB applications

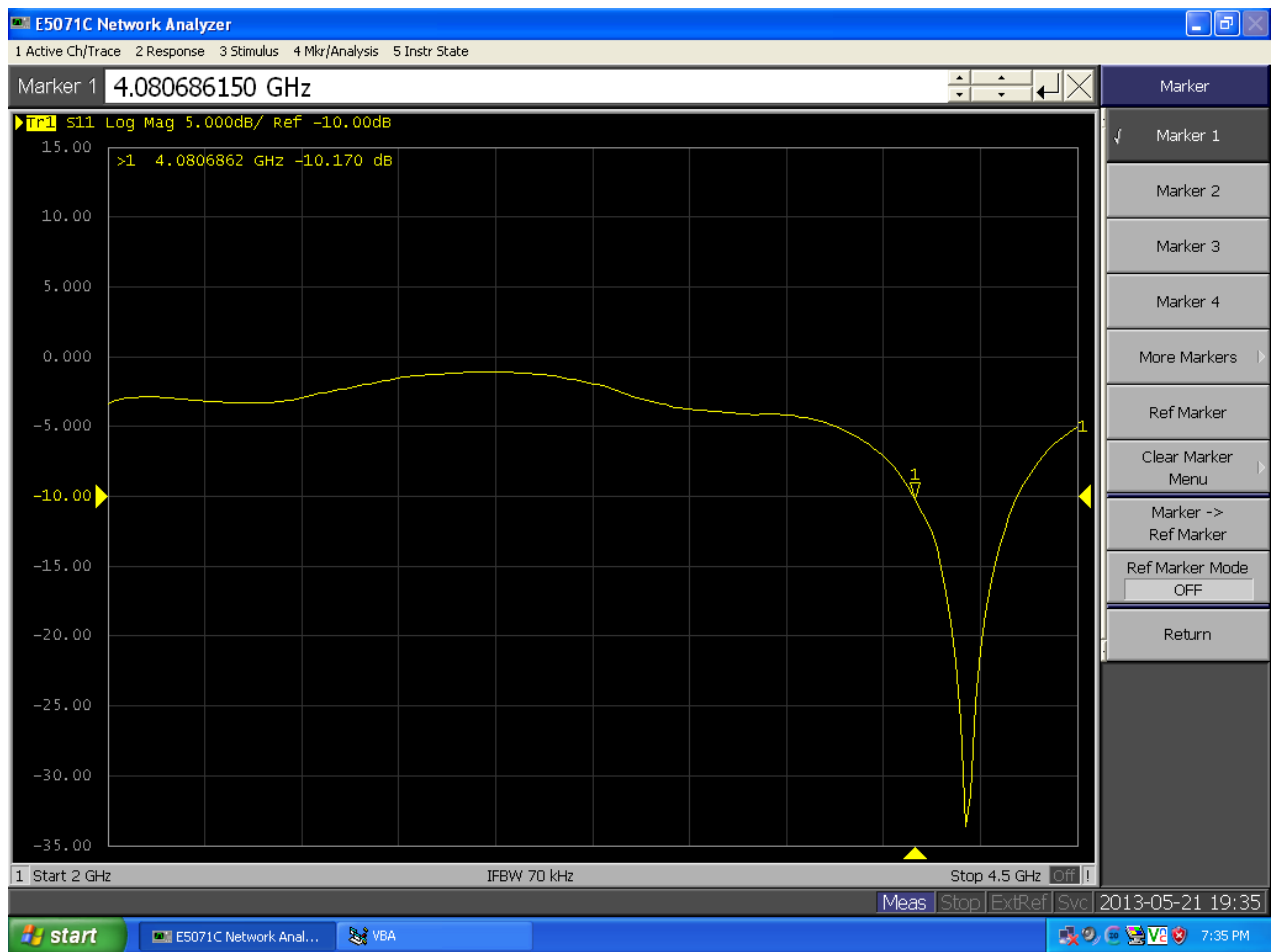


Figure 6.10 Measured return loss of the antenna

The simulated graph of the VSWR of antenna is shown below.

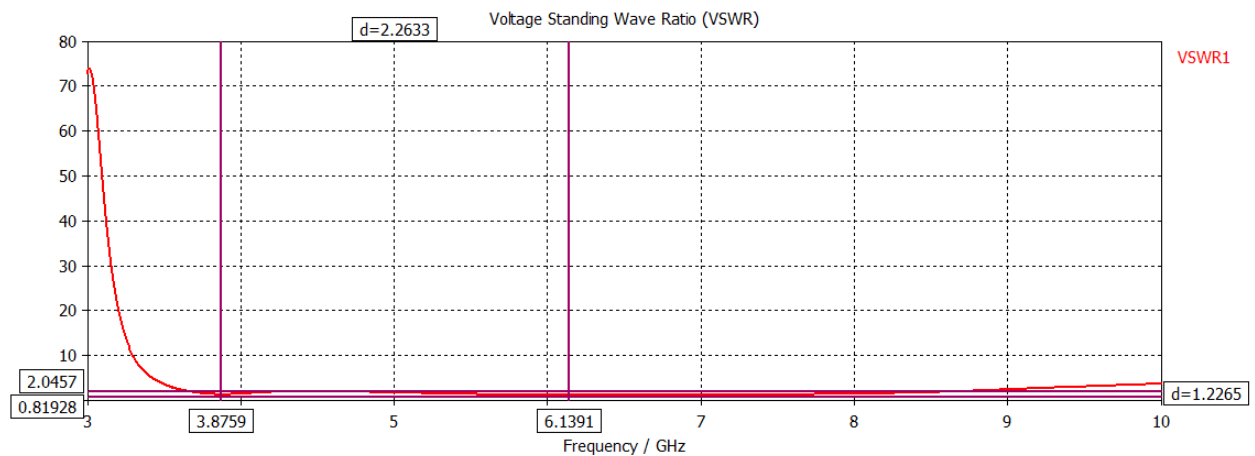


Figure 6.11 VSWR plot of the antenna

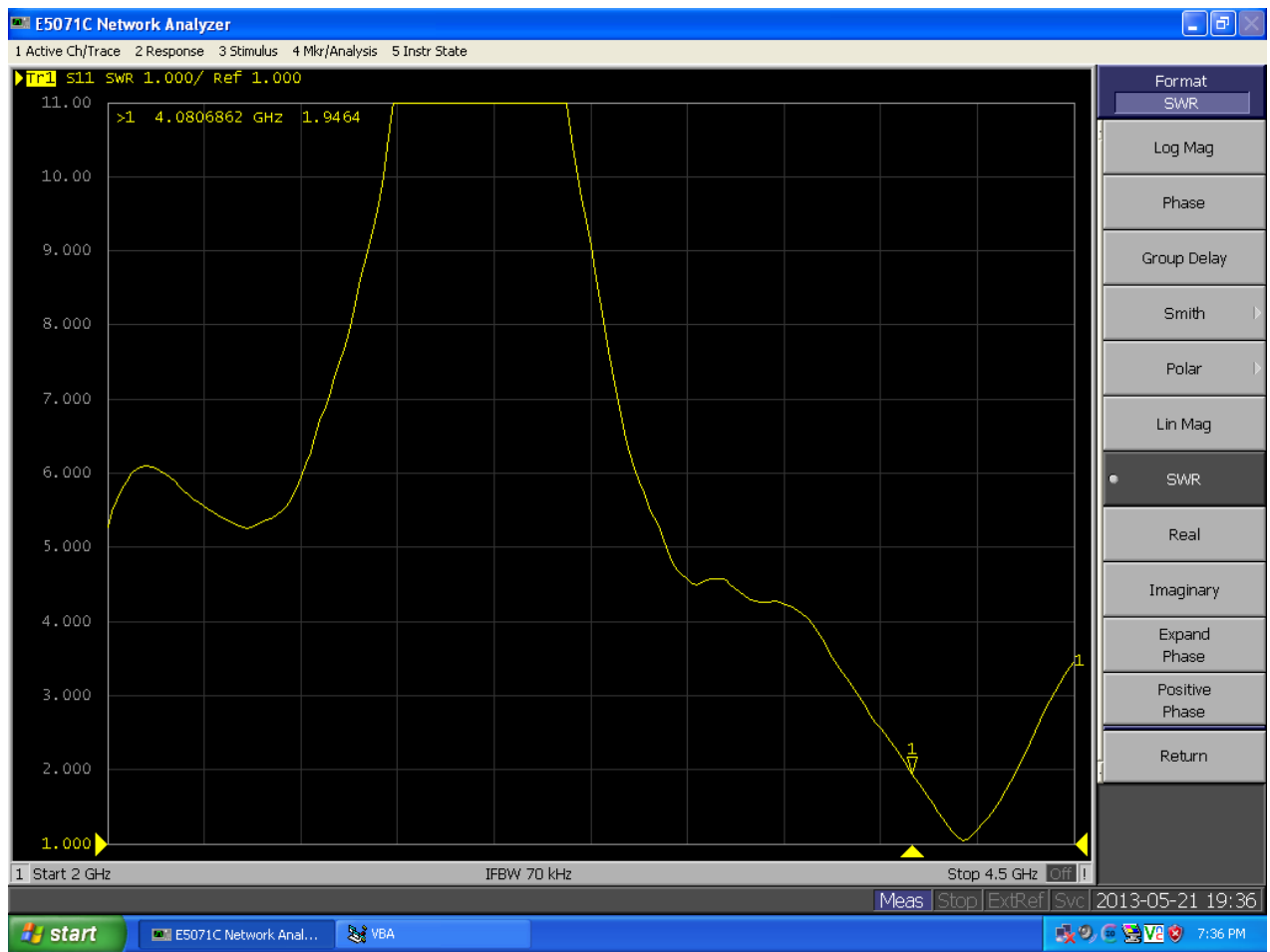


Figure 6.12 Measured value of VSWR

Directivity plot of the antenna is shown below

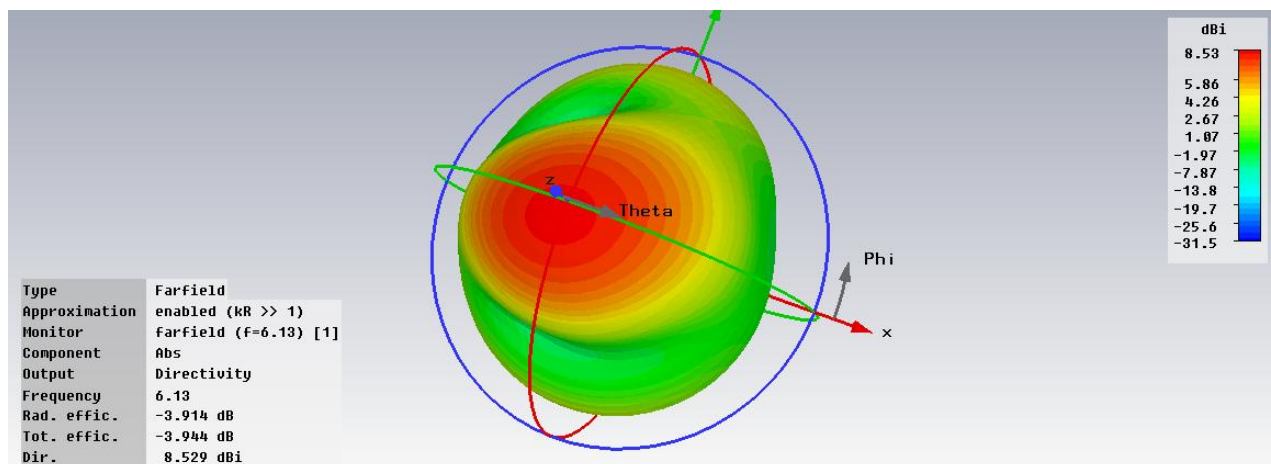
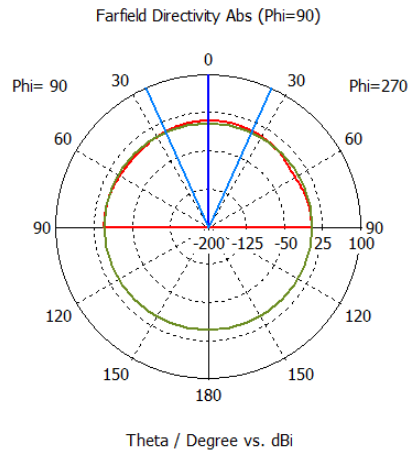


Figure 6.13 Directivity plot of the antenna

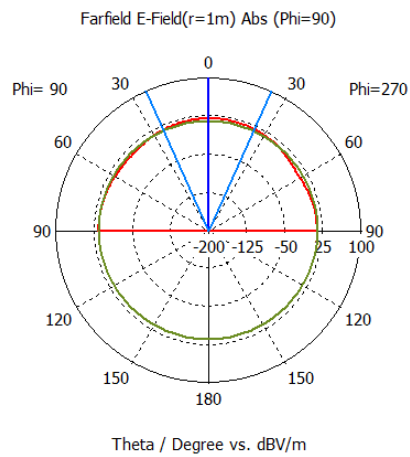


farfield (f=6.13) [1]

Frequency = 6.13
Main lobe magnitude = 8.5 dBi
Main lobe direction = 0.0 deg.
Angular width (3 dB) = 48.7 deg.
Side lobe level = -4.0 dB

Figure6.14 polar representation of directivity

Field pattern plots are also shown below



farfield (f=6.13) [1]

Frequency = 6.13
Main lobe magnitude = 19.4 dBV/m
Main lobe direction = 0.0 deg.
Angular width (3 dB) = 48.7 deg.
Side lobe level = -4.0 dB

Figure 6.15 E- field pattern (phi=90)

CHAPTER 7

CONCLUSIONS AND FUTURE SCOPE

7. 1. CONCLUSIONS

This chapter summarizes and concludes the investigation of Ultra-wide band and Millimeter wave dielectric resonator antenna for wireless applications. Along this research, some analysis techniques for the both micro strip and dielectric resonator antenna have been studied. This thesis emphasizes the main points of the theoretical and practical work performed and conclusions have been drawn based on the results obtained. Results are encouraging.

From the comparative studies it is found that when compared with the micro strip antenna, DRA has a much wider impedance bandwidth. This is because the micro strip antenna radiates only through two narrow radiation slots, whereas the DRA radiates through the whole antenna surface except the grounded part. Moreover the operating bandwidth of a DRA can be varied by suitably choosing the dielectric constant of the resonator material and its dimensions. DRAs have been designed to operate over a wide frequency range (1 GHz to 44 GHz) compared with other antennas existing in the literature. DRAs have a high dielectric strength and hence higher power handling capacity. More over the temperature-stable ceramics enable the antenna to operate in a wide temperature range. The dielectric constant ϵ can be from a range of below 3 up to 100, which allows for a great deal of flexibility when controlling the size and bandwidth. Many of the existing feeding schemes can be used (slots, probes, micro strip, coplanar waveguides, dielectric image guide, etc.). This makes them easy to integrate with existing technologies.

However analytical study of DRA ensures better results compared to micro strip antenna. The efficiency of these two antennas is dependent on radiation resistance and loss resistance. Better efficiency is expected in case of DRA, since the conducting loss is minimum, because of Dielectric material. In this thesis, we have investigated for low-cost, compact size DRAs for UWB and Millimeter wave wireless applications. That is Design and Analysis of a Compact micro strip line Fed DRA for (WLAN) UWB applications, Design and Analysis of I-shape dielectric resonator antenna for millimeter wave applications (This design particularly meant for satellite UPLINK frequencies (31 GHz). Uplink is the portion of a communications link used for the “transmission of signals from an earth terminal to a satellite (or) to an “airborne platform”. The reflection coefficient (S_{11}) is less than -10 dB in all range barring a small and large part of UWB and Millimeter wave frequency range

7.2 FUTURE WORK

Future work can be extended by considering implementation of optimization techniques or the DR antennas. Some analytical models are required to get a clear idea of characteristics of antenna. Good fabrication methods should be followed to minimize the measured errors. Further work can be carried out for different applications with different DRA structures and with different dielectric materials to meet the growing demands in the field of telecommunication in present trend.

Publications:

- [1] Chandra kandula, P K Sahu “*Micro strip line fed novel shaped Dielectric Resonant Antenna for Millimeter wave Applications*”ICRS-
ICMARS, Rajasthan 2011
- [2] Chandra kandula, P K Sahu, Sheeja K L“*Micro strip line fed I-shaped Dielectric Resonant Antenna for Millimeter wave Applications*”
PIERS 2011, Malasiya

References

- [1] C. A. Balanis, "Antenna Theory, Analysis and Design", John Wiley and Sons, 1997.
- [2] K.L. Wong, "Compact and Broadband Microstrip Antennas", John Wiley and Sons, 2002
- [3] Lo, Y.T., Solomon D. and Richards, W.F. "Theory and Experiment on Microstrip Antennas," *IEEE Transactions on Antennas and Propagation*, AP-27, 1979 pp. 137-149.
- [4] Bancroft, R. *Microstrip and Printed Antenna Design* Noble Publishing 2004, chapter 2-3.
- [5] Taga, T. Tsunekawa, K. and Sasaki, A., "Antennas for Detachable Mobile Radio Units," *Review of the ECL, NTT, Japan*, Vol. 35, No.1, January 1987, pp. 59-65.
- [6] A. Sen, J. S. Roy and S. R. Bhadra chaudhuri, "Invest igation on A Dual-Frequency Microstrip Antenna For Wireless applications", *IEEE Xplore*, March, 2009.
- [7] G. Kumar and K.P. Ray, "Broadband Microstrip Antennas", Artech House, 2003.
- [8] K. M. Luk and K. W. Leung, "Dielectric Resonator Antennas", Research Studies Press Ltd Baldock, Hertfordshire, 2003
- [9] Zhi Ning Chen and Michael Y. W. Chia, "Broadband Planar Antennas Design and Applications", John Wiley & Sons Inc., 2006.
- [10] K. R. Carver and J. W. Mink, "Microstrip Antenna Technology," *IEEE Trans. Antennas Propag.*, Vol. AP-29, No. 1, pp. 2-24, January 1981.
- [11] J. R. James and P. S. Hall, *Handbook of Microstrip Antennas*, Vols. 1 and 2, Peter Peregrinus, London, UK, 1989.
- [12] M. Hammoud, P. Poey, and F. Colombel, "Matching the input impedance of a broadband disc monopole", *Electron Lett* 29 (1993), 406-407.
- [13] N. Ghassemi, J. Rashed-Mohassel, and M. H. Neshati, "Microstrip Antenna Design for Ultra Wideband Application by Using Two Slots" *Progress In Electromagnetics Research Symposium*, pp. 169-171, March . 2008.
- [14] K. George Thomas and M. Sreenivasan, "A Simple Ultra-wide band Planar Rectangular Printed Antenna With Band Dispensation", *IEEE transactions on antenna and propagation*, Vol.58, No. 1, January 2010.
- [15] R.D. Richtmyer, "Dielectric Resonators", *J. Appl. Phys.*, Vol. 10, pp. 391-398, June 1939
- [16] S. A. Long, M. W. McAllister and L. C. Shen, "The resonant cylindrical dielectric cavity antenna", *IEEE Trans. Antennas Propag.*, vol. 31, pp. 406-412, May 1983.
- [17] K. W. Leung, K. M. Luk and E. K. N. Yung, "Spherical cap dielectric resonator antenna using aperture coupling," *Electron. Lett.*, vol. 30, No. 17, pp. 1366-1367, Aug. 1994.
- [18] R. K. Mongia, A. Ittipiboon, P. Bhartia and M. Cuhaci, "Electric monopole antenna using a dielectric ring resonator," *Electron. Lett.*, vol. 29, pp. 1530-1531, Aug. 1993.
- [19] Lo H.Y., Leung K.W., Luk K.M. and Yung E.K.N., "Low-profile equilateral triangular dielectric resonator antenna of very high permittivity," *microwave and optical letters*, Vol. 35, No. 25, pp. 2164-65, Nov-16, 2000.

- [20] A. Petosa, "Dielectric Resonator Antenna Handbook", Artech House Publishers, 2007.
- [21] A. A. Kishk and Y. M. M. Antar: *Dielectric Resonator Antennas, from J. L. Volakis: Antenna Engineering Handbook*, Chapter 17, 4th ed., McGraw-Hill, USA; 2007.
- [22] S. A. Long, M. W. McAllister and L. C. Shen, "The resonant cylindrical dielectric cavity antenna", *IEEE Trans. Antennas Propagat.*, vol. 31, pp. 406-412, May 1983.
- [23] Collin, R.E., *Foundations for Microwave Engineering*, New York: McGraw Hill, 1966.
- [24] Mongia, R.K., and A. Ittipiboon, "Theoretical and Experimental Investigations on Rectangular Dielectric Resonator Antennas," *IEEE Transactions on Antennas & Propagation*, Vol. 45, No. 9, Sept. 1997, pp. 1,348-1,356.
- [25] Bit-Babik, G., C. Di Nallo, and A. Faraone, "Multimode Dielectric Resonator Antenna of Very High Permittivity," *IEEE Antennas & Propagation Symposium Digest AP-S 2004*, Monterey, CA, Vol. 2, pp. 1,383-1,386.
- [26] Simons, R.N., and R.Q. Lee, "Effect of Parasitic Dielectric Resonators on CPW/Aperture- Coupled Dielectric Resonator Antennas," *IEE Proceedings Part-H*, Vol. 140, Oct. 1993, pp. 336-338.
- [27] Ittipiboon, A., et al., "Aperture Fed Rectangular and Triangular Dielectric Resonators for Use as Magnetic Dipole Antennas," *IEE Electronics Letters*, Vol. 29, No. 23, Nov. 1993, pp. 2,001-2,002.
- [28] Huang, C.Y., J.Y. Wu, and K.L. Wong, "Cross-Slot-Coupled Microstrip Antenna and Dielectric Resonator Antenna for Circular Polarization," *IEEE Transactions on Antennas & Propagation*, Vol. 47, No. 4, April 1999, pp. 605-609.
- [29] Huang, C.Y., and C.F. Yang, "Cross-Aperture Coupled Circularly-Polarized Dielectric Resonator Antenna," *IEEE Antennas and Propagation Symposium Digest AP-S 1999*, Orlando, FL, pp. 34-37.
- [30] Long, S.A., M.W. McAllister, and L.C. Shen, "The Resonant Cylindrical Dielectric Cavity Antenna," *IEEE Transactions on Antennas & Propagation*, Vol. 31, No. 3, March 1983, pp. 406-412.
- [31] McAllister, M.W., S.A. Long, and G.L. Conway, "Rectangular Dielectric-Resonator Antenna," *IEE Electronics Letters*, Vol. 19, No. 6, March 1983, pp. 218-219.
- [32] Leung, K.W., K.M. Luk, and K.Y.A. Lai, "Input Impedance of a Hemispherical Dielectric Resonator Antenna," *IEE Electronics Letters*, Vol. 27, No. 24, Nov. 1991, pp. 2,259-2,260.
- [33] Kranenburg, R.A., and S.A. Long, "Microstrip Transmission Line Excitation of Dielectric Resonator Antennas," *IEE Electronics Letters*, Vol. 24, No. 18, Sept. 1988, pp. 1,156-1,157.
- [34] Mongia, R.K., A. Ittipiboon, and M. Cuhaci, "Experimental Investigations on Microstrip-Fed Series Dielectric Resonator Antenna Arrays," *Symposium on Antenna Technology and Applied Electromagnetics ANTEM 94*, Ottawa, Canada, Aug. 1994, pp. 81-84.
- [35] Kranenberg, R., S.A. Long, and J.T. Williams, "Coplanar Waveguide Excitation of Dielectric- Resonator Antennas," *IEEE Transactions on Antennas & Propagation*, Vol. 39, No. 1, Jan. 1991, pp. 119-122.
- [36] Harrington, R.F., *Time-Harmonic Electromagnetic Fields*, McGraw-Hill, New York, 1980.